

Reaction of Aniline with FeOCl. Formation and Ordering of Conducting Polyaniline in a Crystalline Layered Host

C.-G. Wu,[†] D. C. DeGroot,[‡] H. O. Marcy,[‡] J. L. Schindler,[‡] C. R. Kannewurf,[‡] T. Bakas,[§] V. Papaefthymiou,[§] W. Hirpo,[†] J. P. Yesinowski,^{†,⊥} Y.-J. Liu,[†] and M. G. Kanatzidis*,^{†,||}

Contribution from the Department of Chemistry and the Center for Fundamental Materials Research, Michigan State University, East Lansing, Michigan 48824, Department of Electrical Engineering and Computer Science, Northwestern University, Evanston, Illinois 60208, Department of Physics, University of Ioannina, 45110 Ioannina, Greece, and Naval Research Laboratory, Code 6120, Washington, D.C. 20375-5342

Received December 5, 1994. Revised Manuscript Received May 18, 1995[®]

Abstract: A detailed study of the intercalative polymerization reaction of aniline with FeOCl, an extensive physicochemical and spectroscopic characterization of the products, and their oxidative behavior in air is presented. FeOCl reacts with excess aniline in CH₃CN at 25 °C, in air, to form black microcrystalline products containing polyaniline (PANI) of the general formula (PANI)_xFeOCl (I). X-ray diffraction from a single crystal of (PANI)_xFeOCl shows that the polymer is intercalated in an ordered fashion that is commensurate with the FeOCl lattice. This ordering causes a doubling of the unit cell in the two in-plane directions (*a*- and *c*-) forming a 2*a* × 2*c* superlattice. The PANI can be extracted from (I) by FeOCl framework dissolution in acid. Molecular weight studies of extracted PANI via gel permeation chromatography (GPC) analysis suggest $\bar{M}_w \sim 6100$ and $\bar{M}_n \sim 3500$ versus $\bar{M}_w \sim 69\,000$ and $\bar{M}_n \sim 7700$ observed for bulk PANI. Chain lengths of PANI in the intralamellar space are shorter than those of bulk PANI but show narrower length distribution. Variable temperature ²H-wide-line NMR of (PANI)_xFeOCl shows that the polymer chains are significantly confined with respect to phenyl ring rotation, but the spectra are influenced by the electron paramagnetism of the host. The (PANI)_xFeOCl was also characterized by infrared spectroscopy, Mössbauer spectroscopy, electron paramagnetic resonance spectroscopy, thermal gravimetric analysis, magnetic susceptibility measurements, and charge-transport measurements. Mössbauer spectroscopy suggests a mixed-valent FeOCl with a Fe²⁺/Fe³⁺ ratio in the material ~1:9. Aerial oxidation of (PANI)_xFeOCl yields an intimate mixture of PANI and β-FeOOH. The PANI after oxidation shows a molecular weight intermediate between that extracted from fresh (PANI)_xFeOCl and bulk PANI. The electrical conductivity of single crystals is 1.5×10^{-2} S/cm and features a thermally activated temperature dependence consistent with a semiconductor. Thermoelectric power measurements show a positive Seebeck coefficient (~10 μV/K) at room temperature which increases steadily with decreasing temperature, reaching the value of 100–400 μV/K at 150 K, consistent with a p-type semiconductor. The charge transport data suggest that in (PANI)_xFeOCl the reduced FeOCl framework dominates the electronic conduction.

Introduction

Electrically conducting polymers have received a great deal of attention due to their promising electrical properties and their potential applications in a variety of devices.^{1,2} A prototype conductive polymer, polyaniline (PANI), known for more than a century,³ has attracted renewed interest during the last decade.⁴ PANI is unique among conducting polymers by virtue of its electrical properties, which can be reversibly controlled by not only changes of its oxidation state but also degree of protonation.^{4,5} Its conducting form exhibits excellent environmental

stability^{4–6} and can be used in organic batteries,⁷ electrochromic displays,⁸ microelectronic devices and sensors,⁹ as a corrosion

(4) (a) Genies, E. M.; Boyle, A.; Lapkowski, M.; Tsintavis, C. *Synth. Met.* **1990**, 36, 139. (b) MacDiarmid, A. G.; Epstein, A. J. *Faraday Discuss. Chem. Soc.* **1989**, 88, 317. (c) Epstein, A. J.; Ginder, J. M.; Zuo, F.; Woo, H. S.; Tanner, B. D.; Richter, A. F.; Angelopoulos, M.; Huang, W. S.; MacDiarmid, A. G. *Synth. Met.* **1987**, 21, 63. (d) MacDiarmid, A. G.; Epstein, A. J. In *Advanced Organic Solid State Materials*; Chiang, L. Y., Chaikin, P. M., Cowan, D. O., Eds.; *Mat. Res. Soc. Symp. Proc.* **1990**, 173, 293.

(5) (a) MacDiarmid, A. G.; Chiang, J. C.; Halpern, M.; Mu, W. L.; D. Somasiri, N. L.; Wu W.; Yaniger, S. I. *Mol. Cryst. Liq. Cryst.* **1985**, 121, 173. (b) MacDiarmid, A. G.; Somasiri, N. L. D.; Salaneck, W. R.; Lundstrom, I.; Liedberg, B.; Hassan, M. A.; Erlandsson, R.; Konrasson, P. *Springer Series in Solid State Science*; Springer: Berlin, 1985; Vol. 63, p 218.

(6) Genies, E.; Syed, A. A.; Tsintavis, C. *Mol. Cryst. Liq. Cryst.* **1985**, 121, 181.

(7) (a) Ohtani, A.; Abe, M.; Higuchi, H.; Shimidzu, T. *J. Chem. Soc. Chem. Commun.* **1988**, 1545. (b) Caja, J.; Kaner, R. B.; MacDiarmid, A. G. *J. Electrochem. Soc.* **1984**, 131, 2744.

(8) (a) Kobayashi, T.; Yoneyama, H.; Tamura, H. *J. Electroanal. Chem. Interfacial Electrochem.* **1984**, 161, 419. (b) MacDiarmid, A. G.; Mu, S. L.; Somasiri, N. L. D.; Wu, G. *Mol. Cryst. Liq. Cryst.* **1986**, 121, 187.

(9) (a) Paul, E. W.; Ricco, A. J.; Wrighton, M. S. *J. Phys. Chem.* **1985**, 89, 1441. (b) Chao, S. Wrighton, M. S. *J. Am. Chem. Soc.* **1987**, 109, 6627. (c) Timoeeva, O. N.; Lubentsov, B. Z.; Sudakova, Ye. Z.; Cheryshov, D. N.; Khidekel, M. L. *Synth. Met.* **1991**, 40, 111.

* Michigan State University.

† Northwestern University.

§ University of Ioannina.

|| Naval Research Laboratory.

¶ Fax 517-353-1793. E-mail: Kanatzidis@cemvax.cem.msu.edu.

® Abstract published in *Advance ACS Abstracts*, August 15, 1995.

(1) (a) *Proceedings of the International Conference on Science and Technology of Synthetic Metals*, (ICSM-92) Göteborg, Sweden, August 1992 [*Synth. Met.* **1993**, Vol. 55] references therein. (b) *Proceedings of the International Conference on Science and Technology of Synthetic Metals*, (ICSM-90) Tübingen, September 1990 [*Synth. Met.* **1991**, Vol. 41–43].

(2) (a) Kanatzidis, M. G. *Chem. Eng. News "Special Report"* **1990**, December 3, p 36. (b) Ferraro, J. R.; Williams, J. M. *Introduction to Synthetic Electrical Conductors*; Academic Press, Inc.: 1987; and references therein.

(3) Letherby, H. *J. Chem. Soc.* **1862**, 15, 161.

inhibitor,¹⁰ acid/base indicator,¹¹ and for optical information storage.¹² The properties of PANI, which is usually prepared by electrochemical¹³ or chemical oxidation of aniline,¹⁴ depend on the method of synthesis.¹⁵ There has been extensive investigation of its chemical structure by IR and Raman spectroscopies,¹⁶ ¹³C and ¹⁵N NMR spectroscopy,¹⁷ TGA/DTA,¹⁸ X-ray photoelectron spectroscopy (XPS),¹⁹ X-ray powder diffraction,²⁰ and via study of model compounds.²¹ However, our understanding of the structure is still fragmentary due to the amorphous or poor crystalline nature and insolubility in common organic solvents. Important structural problems associated with single chain and macromolecular aggregation remain to be solved. The systematic control and modification of the physical, structural, and electronic properties of PANI is an active area of research.²² Goals include the optimization of the charge transport properties and a better understanding of the relationship between electronic and lattice structure. This has been approached by preparing oriented or crystalline polymers. MacDiarmid, Epstein, and co-workers²⁰ studied a microcrystalline form of PANI and proposed a crystal structure, based on X-ray powder diffraction data, similar to that of poly(phenylene-sulfide). Further progress in determining structural details is hampered by the small X-ray coherence length of polycrystalline PANI ($\sim 50\text{--}150$ Å), as larger crystallites are not available. Also key structural features of acceptor-doped PANI were deduced from the single crystal structure determinations of the ClO_4^- and BF_4^- dication salts of $\text{H}(\text{C}_6\text{H}_4\text{NH})_4\text{--C}_6\text{H}_5$, radical cation salts of shorter oligomers and neutral $\text{H}_5\text{C}_6\text{N}=\text{C}_6\text{H}_4=\text{NC}_6\text{H}_5$.²³

One way to obtain orientation of the polymer chains would be to grow them inside a structurally organized host framework.

(10) Mengoli, G.; Musiani, M. M.; Pelli, B.; Vecchi, E. *J. Appl. Polym. Sci.* **1983**, *28*, 1125. (b) Mengoli, G.; Munari, M. T.; Bianco, P.; Musiani, M. M. *J. Appl. Polym. Sci.* **1981**, *26*, 4247.

(11) Syed, A. A.; Dinesan, M. K. *Synth. Met.* **1990**, *36*, 209.

(12) McCall, R. P.; Ginder, J. M.; Leng, J. M.; Coplin, K. A.; Ye, H. J.; Epstein, A. J.; Asturias, G. E.; Manohar, S. K.; Masters, J. C.; Scherr, E. M.; Sun, Y.; MacDiarmid, A. G. *Synth. Met.* **1991**, *41*–43, 1329.

(13) (a) Mohilner, D. M.; Adams, R. N.; Argersinger, Jr., W. J. *J. Am. Chem. Soc.* **1962**, *84*, 3618. (b) Genies, E. M.; Lapkowski, M. *J. Electroanal. Chem.* **1988**, *209*, 97.

(14) (a) Chiang, J.-C.; MacDiarmid, A. G. *Synth. Met.* **1986**, *13*, 193. (b) MacDiarmid, A. G.; Chiang, J.-C.; Richter, A. F.; Somasiri, N. L. D.; Epstein, A. J. Conducting polymers; Alcacer, L., Ed.; Reidel Publications: Dordrecht, 1987; p 105. (c) Pron, A.; Genoud, F.; Menardo, C.; Nechtschein, M. *Synth. Met.* **1988**, *24*, 193.

(15) Lapkowski, M. *Synth. Met.* **1990**, *35*, 169.

(16) Cao, Y.; Li, S.; Xue, Z.; Guo, D. *Synth. Met.* **1986**, *16*, 305.

(17) (a) Kaplan, S.; Conwell, E. M.; Richter, A. F.; MacDiarmid, A. G. *Synth. Met.* **1989**, *29*, E235. (b) Menardo, C.; Nechtschein, M.; Rousseau, A.; Travens, J. P.; Hang, P. *Synth. Met.* **1988**, *25*, 311. (c) Richter, A. F.; Ray, A.; Ramanathan, K. V.; Manohar, S. K.; Furst, G. T.; Opella, S. J.; MacDiarmid, A. G.; Epstein, A. J. *Synth. Met.* **1989**, *29*, E243. (d) Wehrle, B.; Limbach, H.-H.; Mortensen, J.; Heinze, J. *Angew. Chem., Int. Ed. Engl.* **1989**, *28*, 1741.

(18) TGA, Thermal gravimetric analysis; DTA, differential thermal analysis; Wang, S. L.; Wang, F. S.; Ge, X. H. *Synth. Met.* **1986**, *16*, 99.

(19) (a) Tan, K. L.; Tan, B. T. G.; Kang, E. T.; Neoh, K. G. *Phys. Rev.* **1989**, *8070*–*8073*. (b) Salanek, W. R.; Lundstrom, I.; Hjertberg, T.; Duke, C. B.; Conwell, E.; Paton, A.; MacDiarmid, A. G.; Somasiri, N. L. D.; Huang, W. S.; Richter, A. F. *Synth. Met.* **1987**, *18*, 291.

(20) (a) Pouget, J. P.; Jozefowicz, M. E.; Epstein, A. J.; Tang, X.; MacDiarmid, A. G. *Macromolecules* **1991**, *24*, 779. (b) Jozefowicz, M. E.; Epstein, A. J.; Pouget, J. P.; Masters, J. G.; Ray, A.; MacDiarmid, A. G. *Macromolecules* **1991**, *24*, 5863. (c) Fischer, J. E.; Zhu, Q.; Tang, X.; Scherr, E. M.; MacDiarmid, A. G.; Cajipe, V. B. *Macromolecules* **1994**, *27*, 5094.

(21) (a) Wudl, F.; Augus, R. O., Jr.; Lu, F. L.; Allemand, P. H.; Vachon, D. J.; Nowak, M.; Liu, Z. X.; Heeger, A. J. *J. Am. Chem. Soc.* **1987**, *109*, 3677. (b) Baughman, R. H.; Wolf, J. F.; Eckhardt, H.; Lagerstedt, I. *Synth. Met.* **1988**, *25*, 121. (c) Vachon, D.; Augus, R. O.; Lu, F. L.; Nowak, M.; Liu, Z. X.; Schaffer, H.; Wudl, F.; Heeger, A. J. *Synth. Met.* **1987**, *18*, 297.

(22) (a) Epstein, A. J.; MacDiarmid, A. G. *Synth. Met.* **1994**, *65*, 103. (b) Tan, F. R.; Bard, A. J. *J. Electrochem. Soc.* **1986**, *133*, 301. (c) Penner, R. M.; Martin, C. R. *J. Electrochem. Soc.* **1986**, *133*, 310.

The framework could be either three-dimensional, with large oriented tunnels, or two-dimensional, with accessible interlayer space. Recently, conductive polymers were reported to insert in other layered materials such as $\text{V}_2\text{O}_5\text{nH}_2\text{O}$,²⁴ MoO_3 ,^{25,26} UO_2PO_4 ,²⁶ aluminosilicates and clays,²⁷ three-dimensional matrices,²⁸ and zeolites.²⁹ Such materials are unique, with potentially interesting properties of their own not possible from either component separately.

An excellent layered system is FeOCl.³⁰ Growing polymers in FeOCl would result in intercalated compounds with alternating monolayers of polymer chains and FeOCl monolayers. These compounds, if crystalline, may enable us to further characterize the polymer structure by crystallographic and spectroscopic methods. This work follows previous studies of *in situ* intercalative polymerization of pyrrole³¹ and thiophene³² in FeOCl and complements our studies of PANI intercalation in the layered $\text{V}_2\text{O}_5\text{nH}_2\text{O}$ xerogel.^{24a} The products obtained in the latter system are turbostratic, in contrast to the FeOCl-derived products, which are crystalline.

FeOCl consists of edge sharing *cis*- FeCl_2O_4 octahedra with the chlorine atoms lining the van der Waals gap between the layers³⁰ as shown in Figure 1. The *b*-axis, which is perpendicular to the layers, increases upon intercalation as the layers expand to accommodate the guest molecules. Intercalation reactions of FeOCl with a variety of organic compounds such as amine,³³ pyridine,³⁴ tetraselenofulvalene,³⁵ and tetrathiafulvalene³⁵ and organometallic compounds³⁶ are well-known. A preliminary communication on the intercalation of aniline in FeOCl and the properties of the resulting PANI-containing product has appeared.³⁷ Based on experimental data available at that time, we proposed an oxygen-induced phase transformation which produced a more conductive material called the β -phase. Here

(23) (a) Shacklette, L. W. *Synth. Met.* **1994**, *65*, 123. (b) Baughman, R. H.; Wolf, J. F.; Eckhardt, H.; Shacklette, L. W. *Synth. Met.* **1988**, *25*, 121.

(24) (a) Kanatzidis, M. G.; Wu, C. G.; Marcy, H. O.; Kannewurf, C. R. *J. Am. Chem. Soc.* **1989**, *111*, 4139. (b) Wu, C. G.; Kanatzidis, M. G.; Marcy, H. O.; DeGroot, H. O.; Kannewurf, C. R. *Polym. Mat. Sci. Eng.* **1989**, *61*, 969. (c) Liu, Y.-J.; DeGroot, D. C.; Schindler, J. L.; Kannewurf, C. R.; Kanatzidis, M. G. *J. Chem. Soc., Chem. Commun.* **1993**, 593–596.

(25) (a) Nazar, L. F.; Zhang, Z.; Zinweg, D. *J. Am. Chem. Soc.* **1992**, *114*, 6239. (b) Pillion, J. E.; Thompson, M. E. *Chem. Mater.* **1991**, *3*, 777. (c) Nazar, L. F.; Yin, X. T.; Zinweg, D. J.; Zhang, Z.; Liblong, S. *Mat. Res. Soc. Symp. Proc.* **1991**, *210*, 417.

(26) (a) Bissessur, R.; DeGroot, D. C.; Schindler, J. L.; Kannewurf, C. R.; Kanatzidis, M. G. *J. Chem. Soc., Chem. Commun.* **1993**, 687. (b) Liu, Y.-J.; Kanatzidis, M. G. *Inorg. Chem.* **1993**, *32*, 2989.

(27) (a) Mehrotra, V.; Giannelis, E. P. *Solid State Ionics* **1992**, *51*, 115. (b) Mehrotra, V.; Giannelis, E. P. *Solid State Commun.* **1991**, *77*, 155. (c) Soma, Y.; Soma, M.; Harada, I. *Chem. Phys. Lett.* **1983**, *99*, 153.

(28) Nishida, F.; Dunn, B.; Knobbe, E. T.; Fuqua, P. D.; Kaner, R. B.; Mattes, B. R. *Mat. Res. Soc. Symp. Proc.* **1990**, *180*, 747.

(29) (a) Enzel, P.; Bein, T. *J. J. Phys. Chem.* **1989**, *93*, 6270. (b) Bein, T.; Enzel, P. *Synth. Met.* **1989**, *29*, E163. (c) Enzel, P.; Bein, T. *J. Chem. Soc., Chem. Commun.* **1989**, 1326. (d) Caspar, J. V.; Ramamurthy, V.; Corbin, D. R. *J. Am. Chem. Soc.* **1991**, *113*, 600.

(30) Lind, M. D. *Acta Crystallogr.* **1970**, *B20*, 1058.

(31) Kanatzidis, M. G.; Tonge, C. R.; Marks, T. J.; Marcy, H. O.; Kannewurf, C. R. *J. Am. Chem. Soc.* **1987**, *109*, 3797.

(32) Kanatzidis, M. G.; Marcy, H. O.; McCarthy, W. J.; Kannewurf, C. R.; Marks, T. J. *Solid State Ionics* **1989**, *32/33*, 594.

(33) (a) Weiss, A.; Sick, Z. *Naturforsch.* **1978**, *B33*, 1087. (b) Choy, J.-H.; Uh, J.-W.; Kang, J.-K.; Weiss, A.; Rey-Lafon, M. *J. Solid State Chem.* **1988**, *77*, 60. (c) Weiss, A.; Choy, J.-H. Z. *Naturforsch.* **1984**, *B39*, 1193.

(34) (a) Kanamaru, F.; Shimada, M.; Koizumi, M.; Takano, M.; Takada, T. *J. Solid State Chem.* **1973**, *7*, 297. (b) Kanamaru, F.; Koizumi, M. *Jpn. J. Appl. Phys.* **1974**, *13*, 1319. (c) Salmon, A.; Eckert, H.; Herber, R. H. *Chem. Phys.* **1984**, *81*, 5206.

(35) (a) Kauzlarich, S. M.; Teo, B. K.; Averill, B. A. *Inorg. Chem.* **1986**, *25*, 1209. (b) Kauzlarich, S. M.; Stanton, J. L.; Faber, J. Jr.; Averill, B. A. *J. Am. Chem. Soc.* **1986**, *108*, 7946.

(36) (a) Halbert, T. R.; Scanlon, J. *Mat. Res. Bull.* **1979**, *14*, 415–421. (b) Schäfer-Stahl, H.; Abele, R. *Mat. Res. Bull.* **1980**, *15*, 1157.

(37) Kanatzidis, M. G.; Wu, C. G.; Marcy, H. O.; DeGroot, D. C.; Kannewurf, C. R. *Adv. Mater.* **1990**, *2*, 364.

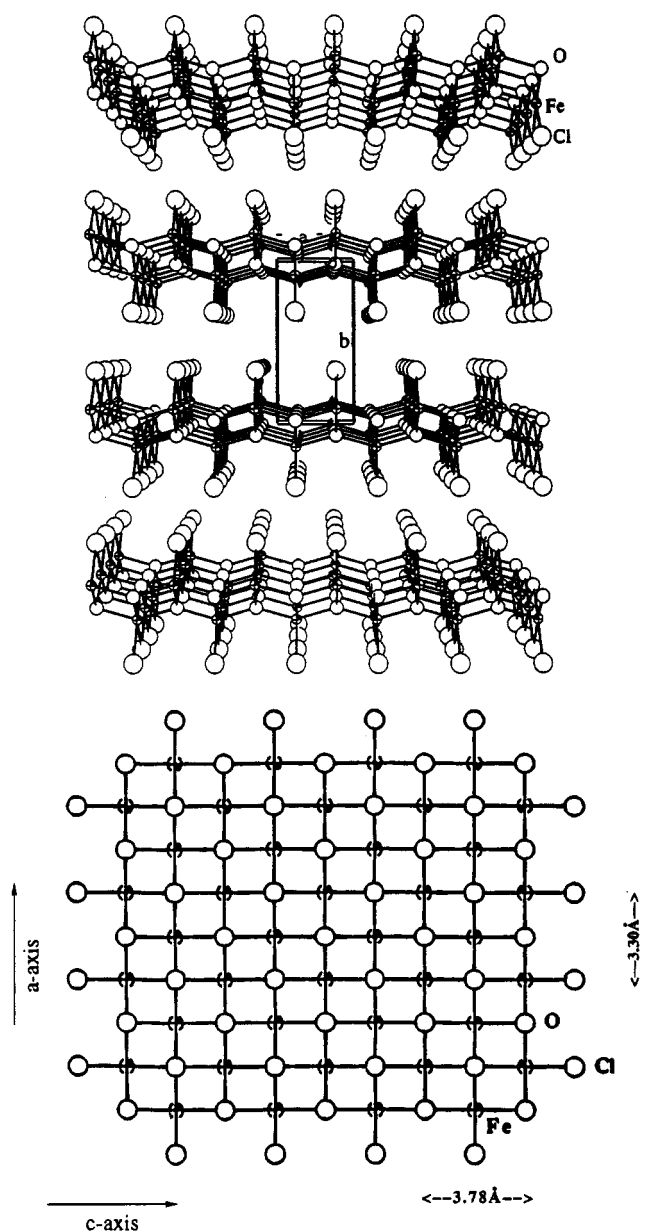


Figure 1. Crystal structure of FeOCl. (top) View perpendicular to the *b*-axis. Large open circles represent chlorine, small open circles represent oxygen atoms, and crossed circles represent iron atoms. (bottom) View down the *b*-axis.

we present a detailed study of the intercalative reaction of aniline with FeOCl, a more complete characterization of the products, their oxidative behavior in air, and an extensive set of spectroscopic and charge transport studies. We also present unambiguous evidence that the β -phase is, in fact, an unusual intimate mixture of β -FeOOH and partially oriented PANI.

Experimental Section

Syntheses. FeOCl was prepared by mixing 9.69 g (59.7 mmol) of FeCl_3 with 7.20 g (45.1 mmol) of Fe_2O_3 in an evacuated Pyrex tube at 380 °C for 4 days. The purple product was washed with acetone to remove excess FeCl_3 and characterized by X-ray powder diffraction. During the reaction, some large single crystals were formed on the edge of the tube away from the bulk material. They were separated from the powder for single crystal reaction studies. Emeraldine salt was synthesized according to a literature procedure.³⁸

(38) MacDiarmid, A. G.; Chiang, J.-C.; Richter, A. F.; Epstein, A. J. *Synth. Met.* 1987, 18, 285 and references therein.

Preparation of Microcrystalline α -(PANI)_xFeOCl, α -I.

α -(PANI)_{0.16}FeOCl. An amount of 60 mL of a 5% aniline solution (32.3 mmol) in acetonitrile was stirred with 0.50 g (4.66 mmol) of FeOCl in air for 1 week. The black shiny microcrystalline product was isolated by filtration, washed with acetone, and dried in vacuo. The yield was quantitative. The intercalation reaction was deemed complete when the (010) peak of the starting FeOCl disappeared from the X-ray powder diffraction pattern. Elemental Anal. Found (%): C, 8.53; H, 1.75; N, 1.59; Fe, 40.12. Calcd (%) for $(\text{C}_6\text{H}_4\text{NH})_{0.16}\text{FeOCl}$: C, 9.45; H, 0.66; N, 1.84; Fe, 45.83.

α -(PANI)_{0.20}FeOCl. An amount of 50 mL of a 4% aniline solution (21.5 mmol) in acetonitrile was mixed with 0.34 g (3.16 mmol) of FeOCl. The mixture was stirred in air for 8 days. The black product was isolated in the same way as above. Elemental Anal. Found (%): C, 11.04; H, 1.59; N, 1.89; Fe, 42.07. Calcd (%) for $(\text{C}_6\text{H}_4\text{NH})_{0.20}\text{FeOCl}$: C, 11.47; H, 0.80; N, 1.84; Fe, 45.83. Other compounds with different stoichiometries were prepared the same way with different reagent ratios. The PANI to FeOCl molar ratio typically varied between 0.16 and 0.28.

Intercalation Reactions with Single Crystals of FeOCl. α -(PANI)_{0.28}FeOCl. An amount of 0.30 g (2.80 mmol) of FeOCl (single crystals) was mixed with 2.00 g (21.51 mmol) of aniline in 50 mL of acetonitrile. Upon standing in air at room temperature without any disturbance for 30 days black shiny crystals of (PANI)_{0.28}FeOCl were obtained. This product was isolated by filtration, washed with acetone, and dried in vacuo. Elemental Anal. Found (%) C, 15.05; H, 1.66; N, 3.29; Fe, 41.50. Calcd (%) for $(\text{C}_6\text{H}_4\text{NH})_{0.28}\text{FeOCl}$ C, 15.18; H, 1.06; N, 2.95, Fe 41.99.

α -(PANI)_{0.23}FeOCl. Single crystals of FeOCl (0.34 g, 3.17 mmol) were mixed with 2.00 g (21.51 mmol) of aniline in 50 mL of acetonitrile. Upon standing in air at room temperature without disturbance for 60 days, black single crystals of (PANI)_{0.23}FeOCl were obtained. The isolation procedure was the same as above. Elemental Anal. Found (%) C, 12.63; H, 1.61; N, 2.76; Fe, 41.70. Calcd (%) for $(\text{C}_6\text{H}_4\text{NH})_{0.23}\text{FeOCl}$ C, 12.91; H, 0.99; N, 2.51; Fe, 43.55.

Isolation of PANI from α -(PANI)FeOCl. An amount of 2.50 g of (PANI)_{0.23}FeOCl was stirred with 400 mL of 2 M HCl(aqueous) at room temperature for 3 days. The black solid was isolated by filtration and washed with H_2O and acetone. It was identified to be PANI by infrared spectroscopy.

Physicochemical Studies. X-ray powder diffraction (XRD) studies were carried out with a Phillips XRG-3000 instrument using Ni-filtered Cu K α radiation. The apparatus was calibrated with FeOCl as an internal standard. The samples were run as powders since pressed pellets show significant preferential orientation. Fourier transform infrared spectra (FTIR) were recorded on pressed KBr pellets using a Nicolet 740 FTIR spectrometer. Thermogravimetric analyses (TGA) were performed with a CAHN TG-121 system using dry oxygen or nitrogen as carrier gas at a flow rate of 120 cm^3/min . The TGA experiments were conducted from room temperature to 950 °C at a linear heating rate of 3 °C/min. Scanning electron microscopy (SEM) [energy dispersive spectroscopy (EDS)] and transmission electron microscopy (TEM) [selected area electron diffraction (SAED) studies], were done with JEOL-JSM 35CF and JEOL-100CX(II) instruments, respectively. Electron paramagnetic resonance (EPR) spectra were recorded with a Varian E-4 spectrometer, using 40 Gauss modulation. The field was calibrated with 2,2-diphenyl-1-picrylhydrazyl (DPPH, $g = 2.0036$). Variable temperature (5–300 K) magnetic susceptibility data were collected on a S.H.E. corporation SQUID system at 5 T applied magnetic field. The samples were placed in a polyethylene bucket. All data were corrected for diamagnetic contributions. The instrument calibration was checked with $\text{HgCo}(\text{SCN})_4$.

Deuterium Nuclear Magnetic Resonance Studies. Perdeuterated aniline (98 atom % deuterium) was purchased from Cambridge Isotope Laboratories. It was converted to the emeraldine salt form by a procedure described earlier.^{19,38} Aniline (*N,N*-*d*₂) was prepared by stirring aniline with 98% D₂O for 2 days. The ²H NMR measurements were carried out on deuterated α -(PANI)FeOCl prepared as described above.

²H NMR spectra were obtained at 9.4 T at a frequency of 61.4 MHz on a Varian VXR-400S solids spectrometer, using a high-power variable-temperature wide-line probe with a 5 mm diameter solenoidal coil that provided 90° pulse lengths of typically 2.8 μ s. The following

composite-pulse quadrupole-echo pulse sequence³⁹ was used in order to obtain more uniform excitation over the wide spectral width:

$$135^\circ_x - 90^\circ_{-x} - 45^\circ_x - \tau - 135^\circ_y - 90^\circ_{-y} - 45^\circ_y - \tau - \text{acquire}$$

The phase of the second half of the sequence was cycled periodically by 180° . A τ delay of 20 μs was used, short enough to minimize distortions and intensity loss due to T_2 relaxation but long enough to reduce (but not completely eliminate) the effects of probe dead time. We note that this sequence refocuses quadrupolar interactions but not paramagnetic dipolar interactions. Given the likely magnitude of the paramagnetic dipolar interactions (discussed later), the absence of a refocusing pulse, for the τ interval used, is likely to produce some phase, and resultant intensity, distortions. Quantitative comparison of the experimental spectra with theoretical simulations is therefore not warranted; however, the changes observed in the spectra with temperature and relaxation recovery delay are nevertheless meaningful. Recycle delays sufficient to allow spin-lattice relaxation were used (typically 1 s and checked with 10 s delay); a spectrum obtained with a long recycle delay of 100 s did not show any difference, indicating the absence of components with long relaxation times. Inversion-recovery experiments were used to measure the spin-lattice relaxation time T_1 , with the initial 180° pulse being a regular pulse. Phasing was carried out on the time domain echo signal to place all of the signal in one channel; the echo maximum was then found by left shifting an appropriate number of points to form a "free induction decay" (fid), which was multiplied by a 2 kHz exponential apodization function and Fourier transformed to yield a properly-phased spectrum. A spectral width of 2 MHz with 16 000 data points was used. Some sample orientation effects, similar to those noted elsewhere in this paper, were observed when tightly compressed cylindrical samples had their compression axis oriented along or perpendicular to the external magnetic field. A looser packing was used for the spectra reported here in an attempt to minimize such effects. We note that the asymmetry observed in the spectra cannot be explained by orientation effects alone.

Gel Permeation Chromatography (GPC). Gel permeation chromatography (GPC) data were obtained by using a Shimadzu LC-10A HPLC system. The column used was a PLgel 10 mm mixed B column, which has an efficiency of more than 35 000 plates per meter. In a typical procedure, 5 mg of emeraldine base was dissolved in 3.0 mL of *N*-methyl-2-pyrrolidinone (NMP). The mixture was then filtered through 4500 Å pore size filter purchased from Phenomenex Inc., Torrance, CA. The column and detector were maintained at room temperature. The injection volume was 10 mL and the flow rate was 0.2 mL/min; a 0.5% LiCl solution in NMP was used as an eluent. Monodisperse polystyrene standards (purchased from Polymer Laboratories Inc., Amherst, MA.) with molecular weights ranging from 580 to 500 800 were used for calibration. The molecular weight of PANI was obtained from a comparison of the retention times of the polymer with the polystyrene standard at the same flow rate and the same eluent.

Mössbauer Spectroscopy. Variable temperature Mössbauer spectra (300–20 K) were obtained using a conventional acceleration spectrometer equipped with a ⁵⁷Co(Rh) source and an Air Products and Chemicals Co. closed-cycle refrigeration system employing helium as a working medium. All isomer shifts are reported with respect to metallic iron at room temperature.

Charge-Transport Measurements. DC electrical conductivity and thermopower measurements were made on polycrystalline compactations of α -I and its oxidized product in pellet form. Conductivity measurements were performed in the usual four-probe geometry with 60- and 25- μm gold wires used for the current and voltage electrodes. Measurements of the pellet cross-sectional area and voltage probe separation were made with a calibrated binocular microscope. Conductivity data were obtained with the computer-automated system described elsewhere.⁴⁰ Thermoelectric power measurements were made by using a slow ac technique⁴¹ with 60- μm gold wires serving to support and conduct heat to the sample as well as to measure the voltage across

(39) Siminovitch, D. J.; Raleigh, D. P.; Olejniczak, E. T.; Griffin, R. G. *J. Chem. Phys.* **1986**, *84*, 2556.

(40) Lyding, J. W.; Marcy, H. O.; Marks, T. J.; Kannewurf, C. R. *IEEE Trans. Instrum. Meas.* **1988**, *37*, 76.

the sample resulting from the applied temperature gradient. In both measurements, the gold electrodes were held in place on the sample with a conductive gold paste.

Conductivity specimens were mounted on interchangeable sample holders, and thermopower specimens were mounted on a fixed sample holder/differential heater. Mounted samples were placed under vacuum (10^{-3} Torr) and heated to 320 K for 2–4 h to cure the gold contacts. For a variable-temperature run, data (conductivity or thermopower) were acquired during both sample cooling and warming to check reversibility. The temperature drift rate during an experiment was kept below 1 K/min. Typically, three to four separate variable-temperature runs were carried out for each sample stoichiometry to ensure reproducibility and stability. At a given temperature, reproducibility was within $\pm 5\%$. The thermoelectric measurements require the production of a slowly varying periodic temperature gradient across the samples and measurement of the resulting sample voltage. Samples were suspended between the quartz block heaters by 60- μm gold wires thermally grounded to the blocks with GE 7031 varnish. The thermopower of a sample is given by eq 1, where the correction for the thermoelectric power of gold is calculated from a polynomial fit to the data of Huebener.⁴²

$$S_{\text{sample}} = (\Delta V_{\text{sample}} / \Delta V_{\text{thermocouple}})(S_{\text{thermocouple}}) + S_{\text{gold}} \quad (1)$$

The magnitude of the applied temperature gradient was generally 3–4 K. Comparisons with temperature-dependent thermopower measurements on standard samples of manganin⁴³ and TEA(TCNQ)₂^{44,45} indicate results with this apparatus to be accurate to better than $\pm 10\%$ between 4.2 and 40 K, where the increased uncertainty is mainly due to the large phonon drag peak of gold. The exact location and magnitude of this peak is known to be dependent on impurity levels, manufacturing methods, etc. for the gold wire.⁴⁶

Results and Discussion

The objective of this study was the detailed characterization of the redox intercalation reaction of aniline with FeOCl and the subsequent polymerization chemistry associated with this system. We begin with a discussion of the synthetic chemistry and polymer characterization, followed by Mössbauer, NMR spectroscopic, magnetic, and charge transport studies of the products. We then discuss the nature of the so-called " β "-phase³⁷ and its ultimate characterization.

Syntheses: The Reaction of Aniline with FeOCl. The reaction of aniline with FeOCl can yield poorly defined products, if not done properly. In one instance it was reported not to occur at all.⁴⁷ For this reason, we investigated the reaction in considerable detail in order to determine the optimum synthetic conditions. Several solvents such as toluene, nitrobenzene, acetone, ethanol, acetonitrile, and even aniline itself were used. We detected no reaction occurring in refluxing nitrobenzene. When the reactions were carried out in refluxing toluene, acetone, ethanol, and aniline, intercalation was observed early in the reaction, but the products decomposed to a brown material before the reaction went to completion. After careful experimentation, we found acetonitrile to be the most suitable solvent. The violet crystals of FeOCl react with excess aniline in CH₃CN at room temperature, in air, to form black microcrystalline products of the general formula (PANI)_xFeOCl. For reasons that will become obvious below we call this α -(PANI)_xFeOCl,

(41) Chaikin, P. I.; Kwak, J. F. *Rev. Sci. Instrum.* **1975**, *46*, 218.

(42) Huebener, R. P. *Phys. Rev.* **1964**, *136*, A1740–A1744.

(43) Christian, J. W.; Jan, J. P.; Pearson, W. B. *Proc. R. Soc. A* **1958**, *213*.

(44) Rathnayaka, K. D. D. *J. Phys. E* **1985**, *18*, 380.

(45) Farges, J. P.; Brau, A. *Phys. Status Solidi B* **1974**, *64*, 269.

(46) (a) Andersen, H. H.; Nielson, M. *Phys. Lett.* **1963**, *6*, 17. (b) Polák, J. *Czech. J. Phys. B* **1963**, *13*, 616. (c) Kopp, J. *Solid State Commun.* **1974**, *14*, 1059.

(47) Maeda, Y.; Yamashita, M.; Ohshio, H.; Tsutsumi, N.; Takashima, Y. *Bull. Chem. Chem. Soc. Jpn.* **1982**, *55*, 3138.

α -I. In general, the mole ratio of aniline to FeOCl must be >8 in order to drive the reaction to completion. Raising the temperature accelerates the reaction but at the same time can accelerate product decomposition. Interestingly, reactions performed under air are much faster than those carried out under nitrogen, indicating that oxygen is involved in the reaction (vide infra). When large single crystals of FeOCl are used, the reaction rate is much slower, but the resulting products contain amounts of PANI similar to the microcrystalline samples. It is nevertheless remarkable that single crystals as long as 0.5 mm can be intercalated completely under the conditions used. Elemental analyses showed varying stoichiometries ($0.17 < x < 0.30$) depending on reaction conditions and the FeOCl particle size. The maximum theoretical x calculated based on the molecular sizes of FeOCl and PANI is ~ 0.3 . Regardless of stoichiometry the products exhibit very similar properties.

Reactions were also carried out in evacuated sealed tubes using ethanol, methanol, acetone, acetonitrile, or dimethoxyethane as a solvent at $80\text{--}110^\circ\text{C}$. Methanol was found to be the most suitable solvent, always yielding single phase products. In other solvents, the products either decomposed or formed multiple phases. The products isolated from sealed tube reactions were black shiny microcrystalline solids with a slightly higher interlayer expansion than those isolated from reactions in open systems. We found that the methanothermally made materials trapped considerable amount of solvent inside, making it difficult to determine the actual polymer content by elemental analysis. These products were also slightly different (electronically and compositionally) from those prepared in acetonitrile at ambient pressure, most likely differing in the degree of reduction of the FeOCl layer and perhaps the degree of polymerization of aniline.⁴⁸ Subsequent studies focused on the products isolated from reactions in air at room temperature using acetonitrile as a solvent, and not on the products of methanothermal reactions.

Infrared Spectroscopy and X-ray Powder Diffraction Studies. Unequivocal evidence for the formation of PANI in the intralamellar space of FeOCl is derived from the FTIR spectra, given in Figure 2, which show the characteristic fingerprint of the emeraldine salt form.⁴⁹ This form is positively charged and requires a counter anion, which in this case is the reduced FeOCl . By comparison, the counterion in bulk emeraldine salt (prepared by aniline oxidation with $(\text{NH}_4)_2\text{S}_2\text{O}_8$ in 0.1 M HCl) is Cl^- . The broad rising absorption at $2000\text{--}4000\text{ cm}^{-1}$ (not shown) which continues into the near-IR is due to the continuum of overlapping electronic transitions, originating from both the mixed-valence FeOCl layer and the intercalated emeraldine salt components. The PANI can be extracted from α -(PANI)_x FeOCl , by digesting the FeOCl framework with 2 M aqueous HCl solution for 20 h. The IR spectrum of the extracted PANI is very similar to an authentic bulk PANI sample. The absorptions of intercalated PANI generally occur at higher frequencies than those of bulk PANI, suggesting that the former probably possesses a lower molecular weight than bulk PANI (vide infra).

Consistent with intercalation, the interlayer spacing of the host lattice expands along the *b* axis. As the reaction proceeds, the XRD peak intensities *Ok0*, *hk0*, *Ok1*, and *hkl* of FeOCl decrease gradually, and new broader peaks appear at lower 2θ

(48) These materials have also undergone metathesis reactions between Cl^- and $-\text{OMe}$ and are of the general formula $(\text{PANI})\text{FeOCl}_{1-x}(\text{OMe})_x$. Kanatzidis, M. G.; Wu, C.-G.; Marcy, H. O.; DeGroot, D. C.; Schindler, J. L.; Kannewurf, C. R. Unpublished results.

(49) (a) Kim, Y. H.; Foster, C.; Chiang, J.; Heeger, A. J. *Synth. Met.* **1988**, 26, 49. (b) Ohira, M.; Sakai, T.; Takeuchi, M.; Kobayashi, Y.; Tsuji, M. *Synth. Met.* **1987**, 18, 347. (c) Snauwaert, Ph.; Lazzaroni, R.; Riga, J.; Verbist, J. J. *Synth. Met.* **1987**, 21, 181.

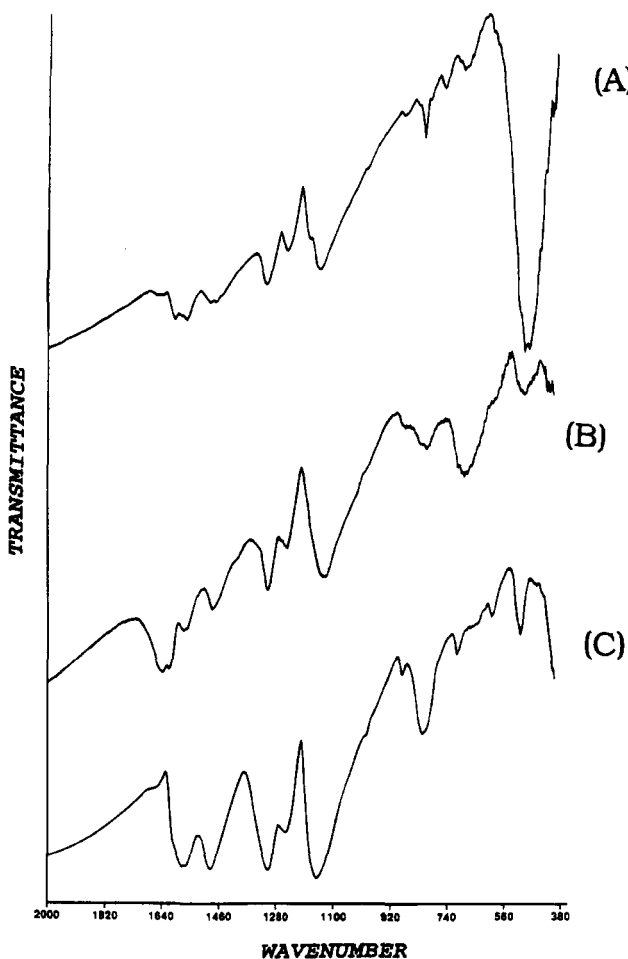


Figure 2. Fourier-transform infrared spectra of (A) α -(PANI)_x FeOCl , (B) β -(PANI)_x FeOCl obtained by oxidation in ambient, and (C) bulk PANI.

angles. At the same time the solid turns black. The reaction was judged complete by the total disappearance of FeOCl *0k0* reflections. During the reaction the basal *0k0* reflections from both the product and the pristine FeOCl coexist, consistent with an *inhomogeneous* intercalation mechanism. The XRD patterns of FeOCl and α -(PANI)_x FeOCl are shown in Figure 3 for comparison. The interlayer spacing of α -(PANI)_x FeOCl is equal to 13.86 \AA , corresponding to an interlayer expansion of 5.94 \AA , sufficient to accommodate the PANI molecules. The magnitude of expansion varies slightly (around 0.6 \AA) between single crystal and powder samples (The interlayer spacing of the single crystals is 14.46 \AA). This variation may be due to irregularities in the arrangement of molecules in the layer gallery, which also can be seen from the larger peak width compared to pristine FeOCl . The magnitude of interlayer expansion suggests the presence of a monolayer of polymer. This also suggests that the twofold axis, bisecting the C—N—C angle, is oriented roughly perpendicular to the FeOCl layers.

α -(PANI)_x FeOCl is moisture sensitive, as prolonged exposure causes the peak intensity at 480 cm^{-1} (Fe—O stretching vibration) in the IR spectrum to decrease. At the same time a new peak develops at $\sim 680\text{ cm}^{-1}$. This indicates significant changes in the FeOCl framework resulting from hydrolysis. No spectroscopic changes are detected under an inert atmosphere.

During intercalation, a few aniline molecules fail to polymerize and are trapped inside the intralamellar space as anilinium (AnH^+) ions. The latter form by reaction of aniline with H^+ released during polymerization. The AnH^+ ions are easily

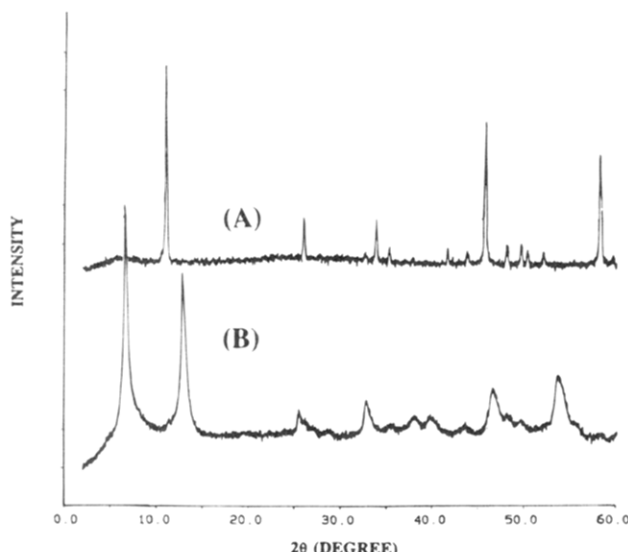
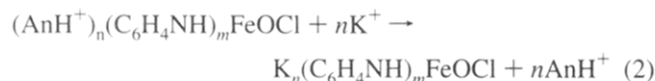


Figure 3. X-ray powder diffraction of (A) pristine FeOCl and (B) α -(PANI)_{0.28}FeOCl.

identified by their characteristic vibrations in the FTIR spectra of the products ($1492, 745, 687\text{ cm}^{-1}$). Subjecting the material to vacuum does not remove the AnH^+ ions. However, upon standing in air, the AnH^+ vibrations gradually disappear without noticeable weight loss, suggesting that the AnH^+ ions polymerize or attach to existing polymer chains in the intralamellar space. This observation implicates oxygen as the electron and proton acceptor. The polymerization of AnH^+ ions can be accomplished by heating the α -(PANI)_{0.28}FeOCl at $140\text{--}200\text{ }^\circ\text{C}$ in air or oxygen for 2 days, as judged by the disappearance of the anilinium vibration peaks from the IR spectrum. The peaks of FeOCl and PANI remain intact. This is the first example of postintercalative oxidative polymerization of a monomer in a layered host induced by molecular oxygen. *This finding raises important implications for the broad applicability of this procedure in producing conjugated polymers in other hosts which contain molecular, but oxidatively polymerizable, guests.*⁵⁰

In order to quantify the presence of anilinium, we attempted ion exchange with K^+ according to eq 2. This is based on the assumption that anilinium, being the smallest species in the intralamellar space and thus the most mobile, would ion-exchange faster than its less mobile oligomers and polymers. Based on nearly complete ion-exchange, the amount of K^+ in the product of eq 2 would correspond to the amount of unpolymerized AnH^+ .⁵¹



The reaction was carried out in CH_3CN using KPF_6 for 20 h. Indeed, ion-exchange is successful as judged by disappearance of the anilinium vibrations in the FTIR spectrum. EDS analysis indicated a molar ratio K/FeOCl of 0.017, which corresponds to $\sim 8\text{--}10\%$ of aniline in the form of AnH^+ in freshly prepared α -I. Interestingly, the interlayer spacing of the K^+ -exchanged product is slightly smaller than that of the starting material by 0.6 \AA . This can be rationalized via a

(50) (a) We have exploited this finding to prepare PANI in UOPO₄-PANI and zirconium phosphate. See ref 26b. (b) Liu, Y.-J.; Kanatzidis, M. G. To be published.

(51) A control experiment in which we attempted K^+ ion-exchange with a sample which did not contain AnH^+ ions (as judged by IR spectroscopy), showed no K^+ incorporation.

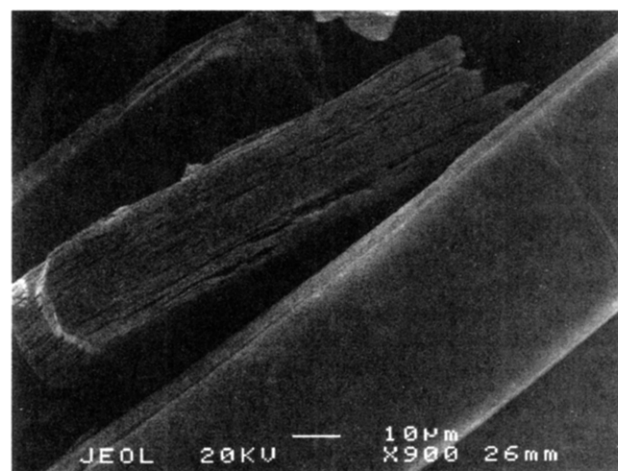
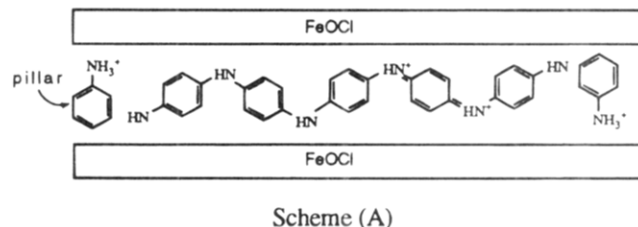


Figure 4. Scanning electron micrographs of α -(PANI)_{0.28}FeOCl.

Scheme 1



structural model in which the anilinium ions are oriented with their C–N bonds perpendicular to the FeOCl layers acting as pillars, while the PANI chains lie parallel to the layers, see Scheme 1. Oxidative coupling changes the orientation of these molecules, thus collapsing the pillars.

Insertion of PANI in FeOCl Single Crystals and In-Plane Structure. Intercalation into single crystal hosts at room temperature is a very slow process; it is seldom complete and usually destroys the crystals. Nevertheless, we still attempted the reaction of FeOCl with aniline to see if similar difficulties existed in this system as well. After several unsuccessful tries, we succeeded in inserting PANI into single crystals of FeOCl by careful slow reaction in air using a CH_3CN solution of aniline. Surprisingly, the resulting compound, α -(PANI)_{0.28}FeOCl, retains significant single crystal character, despite the fact that the overall crystallinity has decreased and most crystals appear multiply cleaved. This can be observed clearly in the SEM photographs shown in Figure 4. The insertion of PANI causes an interlayer expansion of 6.54 \AA .

Examination of crystals of α -I by X-ray diffraction revealed that the crystal quality, though inferior to that of starting FeOCl, was sufficiently good for preliminary X-ray diffraction experiments. Oscillation photographs of such crystals show broad but intense diffraction peaks. The broadest peaks are those of the $0k0$ class of reflections. This is to be expected considering that the FeOCl crystals have undergone topotactic intercalation. The true unit cell of the compound is revealed by the axial X-ray rotation photographs shown in Figure 5.

Interestingly, the diffraction pattern of the hol zone reveals a set of strong reflections associated with the parent $3.30 \times 3.78\text{ \AA}$ cell and a set of several weak reflections half way between the strong ones, suggesting that the periodicity along the a - and c -axes has doubled relative to the original FeOCl unit cell. The new unit cell is orthorhombic, with $a = 6.60\text{ \AA}$, $b = 28.86\text{ \AA}$, $c = 7.56\text{ \AA}$, and $V = 1459\text{ \AA}^3$. The origin of this

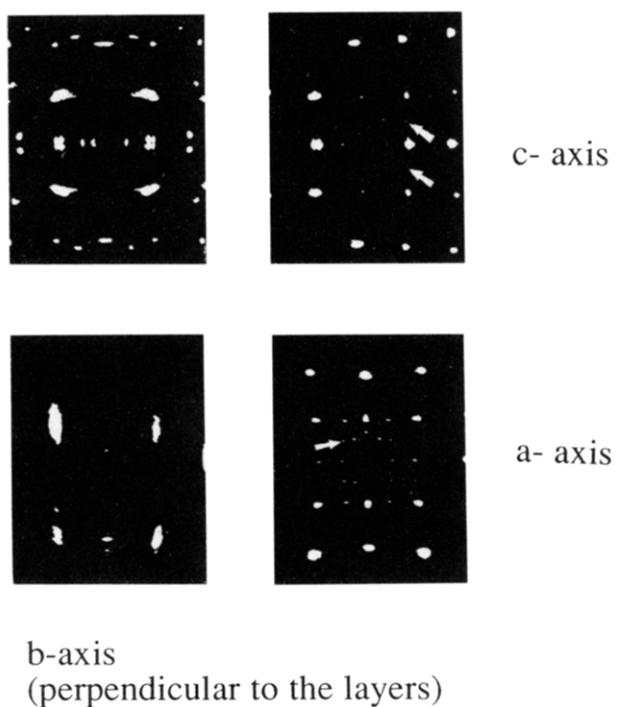
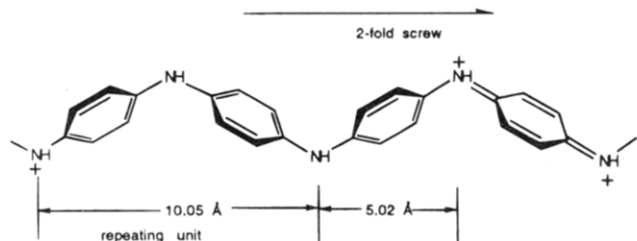


Figure 5. Single crystal X-ray diffraction photographs of α -(PANI) \cdot FeOCl.

Scheme 2



superlattice is due to substantial long-range order of PANI in FeOCl. This long-range order could be achieved by the orientation of the polymer chains along certain crystallographic directions, such that it causes a doubling of the periodicity along the *a*- and *c*-axes. Although the structure of PANI is not yet known in detail, it has been proposed that it is similar overall to that of poly-phenyleneoxide.⁵² This is shown in Scheme 2.

Based on single crystal crystallographic studies of oligoanilines, by Baughman *et al.*,²³ the repeating unit of PANI is estimated to be 10.05 Å (ignoring the details in individual phenyl groups). A 2-fold screw axis runs parallel to the polymer chain with a step of $10.05/2 = 5.02$ Å. By orienting a polymer chain along either the *a*- or the *c*-axes of FeOCl, we see that the repeating unit of the polymer and the inorganic layers are not commensurate. A doubling of the *a*- or *c*-axes cannot be achieved. A close examination of the structural details of FeOCl reveals that the minimum Cl–Cl' distance along the [101] direction (diagonal to the *a*- and *c*-axes) is 5.2 Å, almost one-half of the repeating unit of PANI. By orienting parallel to the [101] (diagonal) direction, see Figure 6, the polymer can spatially match each NH unit with a Cl "partner", see Figure 7. Thus, a diagonal orientation of PANI with respect to the *a*- and *c*-axes of the FeOCl is preferred because it exploits the nearly exact but fortuitous epitaxial relationship of a FeOCl layer and PANI. It also produces a new orthorhombic unit cell with

crystallographic axes $a' = 2a$ and $c' = 2c$.⁵³ Because the doubling of the unit cell is caused by the light carbon and hydrogen atoms, the superlattice reflections would be weak, consistent with the experimental data. In this fashion, the polymer chains can stack side by side lying above every other row of Cl atoms with an interchain distance of ~ 5 Å. One can envision the establishment of H–Cl hydrogen bonding⁵⁴ which can act as an additional stabilizing force. Attempts to obtain infrared spectroscopic evidence for such bonding (using both protonated and deuterated samples) were inconclusive, mainly because that region of the spectrum is dominated by intense electronic absorptions.

The insertion of polyaniline in FeOCl represents a rare example of polymer orientation inside a solid. The exact orientation of the PANI chains in the interlayer space will require the analysis of the X-ray diffraction intensities collected from single crystals. It is also not possible to determine how the PANI chains run from one gallery to the next. The diagonal orientation may change from gallery to gallery in a criss-cross pattern (i.e., parallel to both the [101] and the [101] directions). Furthermore, microtwinning effects may cause a change in the direction of the chains within a single gallery. However, crystal modeling studies show that maximum Cl–H interactions occur only if the diagonal chain orientation alternates in adjacent galleries. This arrangement is shown schematically in Figures 6 and 7.

If indeed the aforementioned epitaxial relationship between atoms of the inorganic layer and atoms in the polymer gives rise to polymer ordering inside FeOCl, then one can envision this occurring in other polymer/inorganic systems by judicious choice of each component. The phenomenon could be termed "endotaxy", indicating the ordering of one material in the interior of another. This is to be contrasted with epitaxy, which is the ordered lattice-matched growth of one material on the surface of another. Previously known superlattice ordering intercalation phenomena involving small ions and molecules can be viewed as examples of endotaxy.⁵⁵

Aerial Oxidation: α -I and the Nature of the " β "-Phase. Early in this investigation, it became evident that oxygen plays an important role in the intercalation of aniline into FeOCl. The first noticeable observation was that the intercalation rates are slower under nitrogen than under air. In fact, reactions carried out under nitrogen often resulted in decomposition before they went to completion. We later determined that decomposition was due to overreduction of FeOCl. Based on our own observations and those reported in the literature, we now recognize that the reductive capacity of this host material is between 0.1 and 0.12e per Fe. Reduction beyond this value results in decomposition.

During the reaction aniline is oxidatively polymerized while FeOCl is reduced. An electron balanced equation for this redox intercalation reaction (assuming that aniline and FeOCl are the

(53) Kanatzidis, M. G.; Wu, C.-G.; Marcy, H. O.; DeGroot, D. C.; Schindler, J. L.; Kannewurf, C. R.; Benz, M; LeGoff, E. *Supramolecular Chemistry in Two and Three Dimensions*; Bein, T., Ed.; ACS Symposium Series **1992**, 499, 194.

(54) Hydrogen bonding between intercalated protonated amines and axial Cl⁻ atoms from inorganic layers has been observed in the $(\text{RNH}_3)_2[\text{CdCl}_4]$ class of compounds: (a) Negrier, P.; Chanh, N. B.; Courseille, C.; Hauw, C.; Meresse, A.; Couzi, M. *Phys. Stat. Solid. (A)* **1987**, 100, 473 (b) Kind, R. *Ferroelectrics* **1980**, 24, 81. (c) Tiecke, B.; Wegner, G. *Angew. Chem. Int. Ed. Engl.* **1981**, 20, 687.

(55) (a) The term endotaxy has been used earlier to describe the ordering effects observed during the diffusion of metals in dense phases such as Co in Si.^{55b} However, the term seems appropriate for use in guest ordering in intercalation compounds, especially when this ordering is caused by guest-host interactions. Fathauer, R. W.; George, T.; Pike, W. T. *J. Appl. Phys.* **1992**, 72(5), 1874–1878. (c) O'Hare, D.; Evans, J. S. O.; Prout, C. K.; Wiseman, P. J. *Angew. Chem. Int. Ed. Engl.* **1991**, 30, 1156.

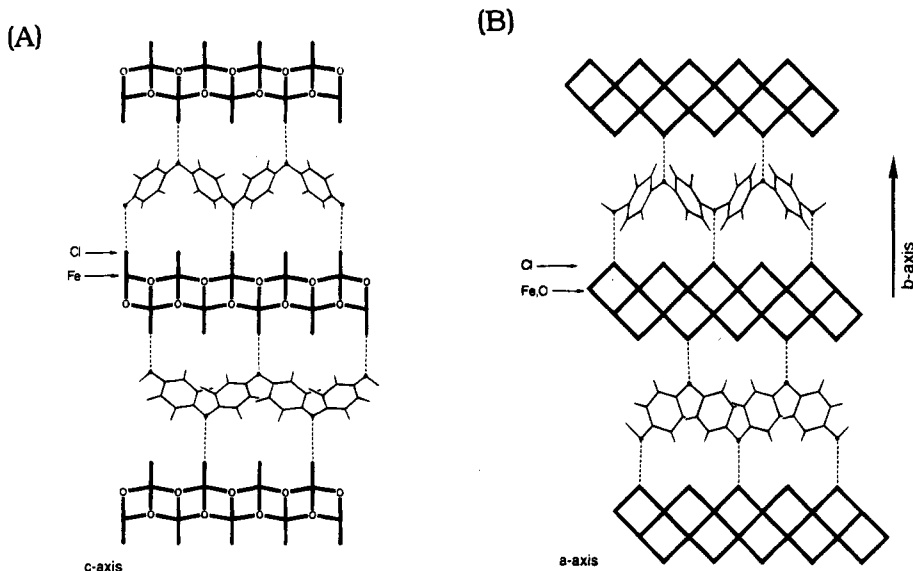


Figure 6. Proposed arrangement of PANI chains in the galleries of FeOCl viewed from two different directions.

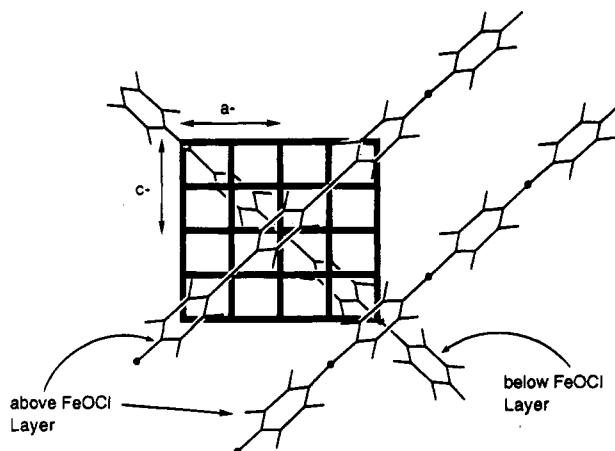
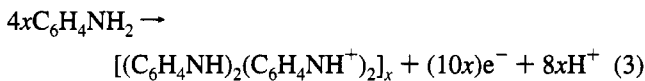


Figure 7. Projection of the relative orientation of PANI chains with respect to a FeOCl layer viewed down the stacking *b*-axis.

only reactants) is shown for each component separately in eqs 3 and 4, with the overall reaction shown in eq 5.



Equation 5 demands that all protons released from aniline be retained in the product and that FeOCl accept all transferred electrons. Thus, a product with 0.20 equiv of aniline per FeOCl should contain iron in the $\sim +2.5$ oxidation state. In other words, 50% of the Fe^{3+} sites should be reduced to Fe^{2+} . This is contrary to two experimental facts: (a) the quantitation of $\text{Fe}^{2+}/\text{Fe}^{3+}$ by Mössbauer spectroscopy shows that only $\sim 10\%$ of the Fe atoms are in the Fe^{2+} state, regardless of stoichiometry (see below) and (b) the inability of the FeOCl lattice to sustain more than $\sim 10\%$ of the Fe atoms in a +2 state without structural decomposition.⁵⁶ The fact that no H^+ ions were detected in

the products suggests that only part of the electrons are transferred to the host, while the rest end up elsewhere. The latter is apparently molecular oxygen, which acts not only as electron acceptor but also as proton acceptor, forming either H_2O or H_2O_2 . Oxygen could participate in the reaction by either oxidizing generated Fe^{2+} , thus increasing the oxidation state of FeOCl, or by oxidizing directly intermediate aniline oligomers which themselves might be more reducing than aniline.⁵⁷

Upon standing in air for several months, α -(PANI)_xFeOCl gradually transforms to a different product. This change is associated with considerable changes in the physicochemical and electrical properties of the material. No change is observed when the samples are stored in evacuated sealed tubes. We reported earlier that this amounted to a phase transition from α -I to β -I. Here we would like to specifically define the so called α - and " β "-phases. Freshly prepared (PANI)_xFeOCl is defined as the α -phase. The material obtained upon standing in air for a month is defined as the " β "-phase. At this stage, the product is weakly crystalline or amorphous. Based on the data given below, the phase change can be rationalized by assuming that in the intralamellar space the PANI chains couple further to form higher molecular weight polymer. However, attempts to accelerate the transformation by heating the sample under an oxygen flow at 140–200 °C were not successful, presumably due to the absence of water. Furthermore, independent of polymer oxidation, a concurrent hydrolysis takes place at the FeOCl framework. The hydrolysis is not abrupt but slow and continuous. As the oxidation proceeds, we observe the slow but steady disappearance of diffraction lines of α -I and the appearance of some new weak diffraction lines. For simplicity, we consider to have obtained the " β "-phase after the complete fading of the IR peak at 480 cm^{-1} , which is due to vibrations in the FeOCl framework in α -I. The infrared spectra of α -I and " β "-phase of (PANI)_xFeOCl are shown in Figure 2. The term " β "-phase is used loosely since *this material is not a pure compound* but a mixture of two phases (vide infra). The full characterization of both phases was accomplished with a variety of experimental techniques described below.

PANI Extracted from α -I and " β "-I versus Bulk PANI and Molecular Weight Studies.

The products extracted from

(56) Meyer, H.; Weiss, A.; Besenhard, J. O. *Mat. Res. Bull.* 1978, 13, 913–920.

(57) (a) Wei, Y.; Jang, G.-W.; Chan, C.-C.; Hsueh, K. F.; Hariharan, R.; Patel, S. A.; Whitecar, C. K. *J. Phys. Chem.* 1990, 94, 7716. (b) Wolf, J. F.; Forbes, C. E.; Gould, S.; Shacklette, L. W. *J. Electrochem. Soc.* 1989, 136, 2887.

α -(PANI)_xFeOCl and the " β "-phase will be referred to as α - and " β "-PANI. α -PANI differs from bulk PANI in several respects. First, in its emeraldine base form, it is soluble in tetrahydrofuran (THF) and dimethylformamide (DMF), while the corresponding bulk PANI is not. Second, the salt form of the extracted PANI has room temperature conductivity of 0.1 S/cm compared to 1–5 S/cm for the corresponding bulk emeraldine salt. These data suggest that the intercalated PANI consists of significantly shorter chains than bulk PANI and thus has a correspondingly smaller MW. This is rationalized by the slower kinetics of aniline chain-growth in the constrained environment of FeOCl, which results in relatively short chains. Thermal gravimetric analysis shows that α -PANI decomposes at the lowest temperature of 220 °C, while " β "-PANI starts to decompose at 260 °C, consistent with the smaller MW of the former. By comparison bulk PANI shows abrupt weight loss at ~300 °C due to decomposition.

Estimates of the molecular weight of the polymer were obtained with gel permeation chromatography (GPC) analysis. GPC graphs were obtained by using a 0.5% LiCl solution of NMP as an eluent at room temperature. The MW distribution observed in the GP chromatographs of α -PANI was bimodal with one relatively sharp, intense band with maxima corresponding to $M_w \sim 6100$ and $M_n \sim 3500$ and a weak band arising from a oligomeric fraction with molecular weight of 650. " β "-PANI showed only one GPC band with $M_w \sim 15\,000$ and $M_n \sim 5900$. For comparison, under the same experimental conditions bulk PANI gave $M_w \sim 69\,000$ and $M_n \sim 7700$. It is noteworthy that the polydispersity index (M_w/M_n) of α -PANI is markedly smaller than that of bulk PANI. The degree of polymerization (based on the formula $(-\text{C}_6\text{H}_4\text{NH}-)_n$) according to M_n is estimated at $n \sim 38$ for α -PANI and at $n \sim 65$ for " β "-PANI. From these data we can conclude that while chain growth in the intralamellar space is greatly slowed, it is more orderly, resulting in polymer of lower chain-length polydispersity than bulk PANI. The presence of the oligomer with MW ~650 (perhaps a heptamer) is attributed to kinetic trapping of oligomers in small regions surrounded by long polymer chains.

Thermogravimetric Analysis (TGA). The TGA diagram of α -(PANI)_xFeOCl, under nitrogen, shows a two step decomposition pattern. A slow weight loss from 50 °C to 625 °C is associated with loss of volatile organic products, while the sharp weight loss commencing at around 625 °C is due to the volatilization of FeCl₃ from the layered framework. In contrast, FeOCl is stable up to 540 °C before it decomposes to Fe₂O₃ and FeCl₃ in one step. The thermal stability of α -(PANI)_xFeOCl decreases significantly when oxygen is used as a carrier gas. Under nitrogen, α -(PANI)_xFeOCl loses weight slowly from 50 °C to 350 °C, while a faster weight loss is observed from 350 °C to 500 °C. On the other hand, the " β "-phase shows continuous weight loss from 50 °C to 500 °C.

²H-NMR Spectroscopic Studies. A variety of solid-state NMR approaches have been used to study the various forms of PANI. The "high-resolution" method of cross-polarization magic-angle-spinning (CP-MAS-NMR) has been used for both the ¹³C^{58,59} and ¹⁵N¹⁷ isotopes; however, obtaining detailed information about chemical structure is difficult, due to the rather large inhomogeneous line widths observed. Detailed information about temperature-dependent motional dynamics, specifically "flipping" of deuterated aromatic rings, was obtained using ²H quadrupolar-echo spectra, and variations in the fraction of

rings undergoing flips were observed with temperature and sample type.⁵⁸

In this study we used ²H quadrupolar-echo NMR to investigate deuterated PANI intercalated into FeOCl. In diamagnetic solids deuterium NMR spectra are generally interpreted in terms of a nuclear quadrupole coupling constant (NQCC) and its corresponding asymmetry parameter η . These two parameters, while characteristic of the chemical type (bonding environment) of the deuterium atom, are also affected by molecular motions that result in motional averaging. The deuterium chemical shift anisotropy is generally negligible. The result is a spectrum that is symmetric about its center frequency, even in the presence of partial orientation effects. However, paramagnetic species in proximity to the deuterium atoms can lead to pronounced asymmetries in the spectra resulting from the through-space dipolar interactions between the Curie moments of the (rapidly-relaxing) electrons of the paramagnetic species and the deuterium atoms.⁶⁰ The dipolar interactions between the unpaired electrons of one or more paramagnetic ions and a deuterium nucleus have the same effect on the deuterium spectrum as a (in general nonaxially symmetric) deuterium chemical shift tensor. Powder deuterium line shapes resulting from combined quadrupolar and chemical shift anisotropy terms have been previously discussed.⁶¹ However, since the Curie moments of paramagnetic samples are temperature (and magnetic field) dependent, they can lead to temperature-dependent spectra even in the absence of motional dynamics.

Deuterium quadrupolar-echo spectra of perdeuterated bulk PANI were obtained as a function of temperature. The spectra from 188 to 298 K exhibit a characteristic deuterium powder pattern with $\eta \sim 0$ and NQCC ~168 kHz, similar to previous observations at 300 K.⁵⁸ From 373 to 423 K in addition to this pattern there is a fairly sharp doublet with a splitting of 31.3 kHz and a sharp central peak that grow in; the inner doublet is presumably due to the presence of groups undergoing ring flips, as observed previously,⁵⁸ whereas the sharp central peak presumably arises from some species undergoing isotropic reorientation. We have ignored so far the deuterium atoms attached to nitrogen atoms, which have not been previously studied in PANI. The ²H quadrupolar-echo NMR of amino group deuterons in *p*-nitroaniline has been reported to be distorted due to the presence of heteronuclear dipolar couplings to ¹⁴N, and signal intensity can be lost due to transverse deuterium relaxation arising from the ¹⁴N relaxation.⁶² In addition, resonance offset effects from the deuteron chemical shift tensor will lead to distortions in quadrupolar echo spectra obtained in high magnetic fields and without 180° refocusing pulses.⁶³ We were unable to obtain any spectra (visible above the artifacts due to probe ringdown) of specifically N-deuterated PANI with the normal pulse interval of $\tau = 20\ \mu\text{s}$. By increasing τ to 100 μs , a weak powder pattern characteristic of a small η value (~0) with a splitting between the "horns" of ~130 kHz could be observed; in addition, a sharp central peak appeared. We may speculate that the sharp peak arises from some small fraction of deuterons undergoing nearly isotropic motion due to hopping between different sites and that it also appears as the central sharp peak in the spectrum of the perdeuterated salt.

(58) (a) Woehler, S. E.; Wittebort, R. J.; Oh, S. M.; Hendrickson, D. N.; Inniss, D.; Strouse, C. E. *J. Amer. Chem. Soc.* **1986**, *108*, 2938. (b) Woehler, S. E.; Wittebort, R. J.; Oh, S. M.; Kambara, T.; Hendrickson, D. N.; Inniss, D.; Strouse, C. E. *J. Am. Chem. Soc.* **1987**, *109*, 1063.

(61) Torgeson, D. R.; Schoenberger, R. J.; Barnes, R. G. *J. Magn. Reson.* **1986**, *68*, 85–94.

(62) Kennedy, M. A.; Vold, R. R.; Vold, R. L. *J. Magn. Reson.* **1991**, *91*, 301–315.

(63) Siminovitch, D. J.; Rance, M.; Jeffrey, K. R.; Brown, M. F. *J. Magn. Reson.* **1984**, *58*, 62.

(58) Kaplan, S.; Conwell, E. M.; Richter, A. F.; MacDiarmid, A. G. *Macromolecules* **1989**, *22*, 1669.

(59) (a) Kaplan, S.; Conwell, E. M.; Richter, A. F.; MacDiarmid, A. G. *J. Am. Chem. Soc.* **1988**, *110*, 7647. (b) Devreux, F.; Bidan, G.; Syed, A.; Tsintavis, C. *J. Phys.* **1985**, *46*, 1595.

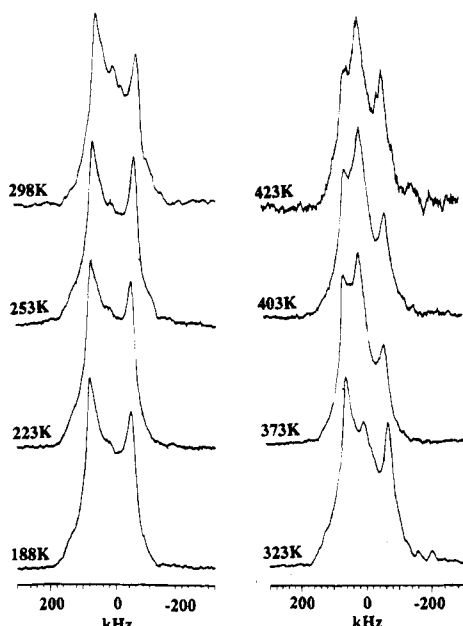


Figure 8. Quadrupolar echo ^2H -NMR spectra of α -(PANI)_{0.20}FeOCl as a function of temperature. All spectra were recorded with a repetition delay of 1 s. Number of scans was 3000 for 188, 223, and 253 K; 5000 for 323 and 373 K; 900 for 403 K; and 150 for 423 K.

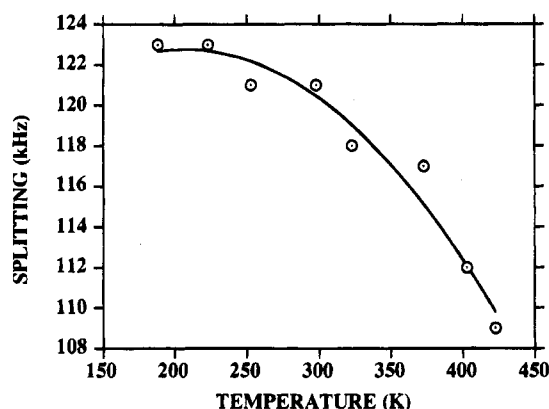


Figure 9. The dependence of the splitting between the outer "horns" of the ^2H -NMR spectra of α -(PANI)_{0.20}FeOCl as a function of temperature. The line through the points serves as a guide to the eye.

Deuterium composite pulse quadrupolar-echo spectra for the perdeuterated PANI intercalated into FeOCl (i.e., α -(PANI)_xFeOCl) are shown in Figure 8 from 188 to 423 K. Additional experiments suggest that at temperatures up to at least 348 K the observed changes are reversible, but by 423 K the spectra obtained after cooling the sample back to room temperature differ from the original room temperature spectra, primarily in a decreased intensity of the two outer "horns". Whether these irreversible changes are due to deintercalation, further reaction (oxidation, polymerization) of the polymer in the FeOCl host or structural reorganization of the intercalated polymer is not known. The splitting between the two most intense features in the spectra decreases gradually from approximately 123 kHz at 188 K to 109 kHz at 423 K, see Figure 9.

The specifically deuterated PANI(*N,N-d*₂)-FeOCl sample failed to yield a ^2H quadrupolar-echo spectrum at room temperature, even after 3000 acquisitions with a τ delay of 20 μs . This could be due to a short T_2 relaxation time, possibly due to motions of the amino deuteron and/or paramagnetic effects; it is interesting that the correspondingly-labeled bulk emeraldine salt of PANI also yielded a very weak signal. Another possibility is that the signal is inhomogeneously

broadened by paramagnetic centers (either in the host or in the polymer chain). Regardless of the reasons for the absence of a signal from the amino deuteron, we will assume in the discussion below that the ^2H spectra of the perdeuterated PANI-FeOCl sample at all temperatures arise only from the ring (aromatic) deuterons and not from the deuterons on the amino group.

The ^2H spin-lattice relaxation behavior in an inversion-recovery experiment for PANI-FeOCl at room temperature could not be fit to a single exponential recovery. Although there are well-known difficulties with extracting multiple exponential time constants from such data,⁶⁴ it is possible to determine two widely-different time constants. Experimental peak intensities at various portions of the spectrum were visually fit to a theoretical curve for two components of differing percentages (summing to 100%). They possessed different T_1 values, with a suitable correction factor allowing for the lesser intensity of the $\tau \sim 0$ spectrum compared to the $\tau \gg T_1$ spectrum (due to B_1 inhomogeneity). No marked differences due to the frequency of the peak chosen were noted (see 'below'). A reasonable fit for τ values ranging from 0.5 ms to 1.0 s was obtained for a biexponential fit having ca. 50–55% of a slow-relaxing component having a T_1 of 0.3 s and 45% of a fast-relaxing component having a T_1 of 0.01 s.

A plausible explanation of the biexponential relaxation behavior is the presence of two different types of deuterons, each with a single-exponential relaxation but with different T_1 time constants.⁶⁵ This explanation lends itself to an assignment of the slow and fast relaxing components to the two inequivalent ring deuterons that would be expected for the aromatic ring. The two types of deuterons may differ in their distance from a $\text{Fe}^{2+}/\text{Fe}^{3+}$ paramagnetic center that serves to relax the nuclear spins. One consequence of this interpretation is that it should be possible to obtain the *spectrum* of each component separately by the null-method, using a τ recovery delay in the inversion recovery pulse sequence equal to $\ln(2)xT_1$ (other component).

This experiment was carried out on a sample that did not have the very intense peak on the left seen for the sample above (which was used for the T_1 measurement). The spectrum of the fast-relaxing component, obtained with $\tau = 0.21$ s, shown in Figure 10A shows two pronounced "horns" with a splitting of ~120 kHz with additional unsymmetrical intensity on the downfield side. The spectrum of the slow-relaxing component obtained with $\tau = 0.0069$ s, shown in Figure 10B is somewhat different, having a flat slanting profile rather than a pronounced dip between the position of the two horns in the other spectrum and having less intensity outside these horns.⁶⁶

The asymmetric features of the spectra discussed above and the sizable downfield shift of the center of gravity of the spectrum of approximately 20 kHz (330 ppm) measured relative to D_2O are too large to be due to a "normal" chemical shift anisotropy of the deuteron. They most likely arise from a through-space dipolar interaction (pseudocontact shift) with

(64) Brown, R. J. S. *J. Magn. Reson.* 1989, 82, 539. Whittall, K. P.; MacKay, A. L. *J. Magn. Reson.* 1989, 84, 134.

(65) Relaxation behavior that does not follow a single-exponential recovery could be due to a number of causes. Dilute paramagnetic centers directly relaxing nuclei that are not in spin diffusion contact with each other result in a recovery curve having a $(1 - \exp(-\tau/T_1)^{1/2})$ dependence.^{65a} This is not what we observe; the fact that the $\text{Fe}^{2+}/\text{Fe}^{3+}$ paramagnetic centers in our system are not dilute mean they do not produce the distribution of radial distances from the paramagnetic centers that result in the above dependence. Nonexponential relaxation at short times has been observed in the conducting polymer polythiophene, where it was attributed to the effects of heterogeneous doping.^{65b} The differences between the observed and predicted dependencies, on the one hand, and a single exponential, on the other hand, were rather small, although significant. (a) Tse, D.; Hartmann, S. R., *Phys. Rev. Lett.* 1968, 21, 511. (b) Le Guennec, P.; Nechtschein, M.; Travers, J. P. *Phys. Rev. B* 1993, 47, 2893.

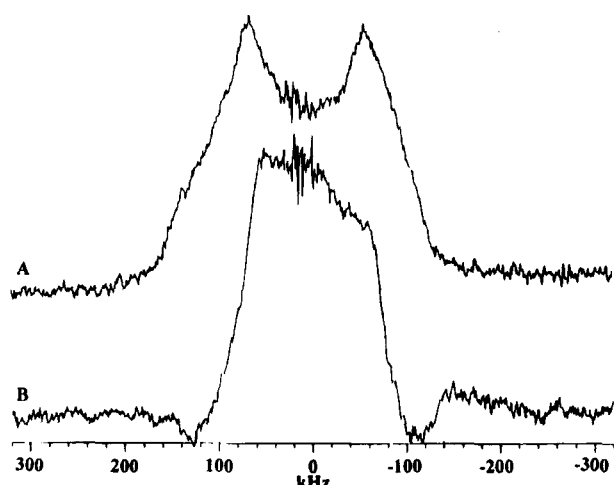


Figure 10. Inversion recovery quadrupolar echo ^2H NMR spectra of (A) the fast relaxing component obtained with $\tau = 0.21$ s, number of scans was 1900, and (B) the slow relaxing component obtained with $\tau = 0.0069$ s, number of scans was 1800. (See text for explanation.)

unpaired electrons in the paramagnetic FeOCl host. We note the possibility of a Knight shift⁶⁷ arising from the metallic character of the guest polymer might also be invoked to explain the results. Whether a Knight shift would possess sufficient anisotropy to account for the presently observed asymmetry is uncertain. Normally, Knight shifts follow the well-known Korringa relationship,⁶⁷ which implies that the product of the spin-lattice relaxation time T_1 and the absolute temperature T is a constant related to the inverse square of the Knight shift. However, such a test is impractical in our system, because of the biexponential character of relaxation and the presence of thermally-active molecular motion (see below). Nevertheless, we can consider the effects of the paramagnetic dipolar interactions qualitatively, in comparison with previous work,⁶⁰ where a magnetic moment μ_{eff} of $5.9 \mu_B$ in a magnetic field of 5.9 T yielded a paramagnetic dipolar coupling at room temperature of ca. 15 kHz. The paramagnetic centers were assumed to be about 6 \AA from the deuterium and made an angle of 21° . If we take into account our higher field strength but lower *bulk magnetic moment* of $2.8 \mu_B$ in α -I, we obtain roughly the same magnitude of paramagnetic dipolar coupling for the same distance to a “reduced” spin-only magnetic moment. Since molecular models show that the aromatic ring deuteron in α -I is $\sim 4 \text{ \AA}$ from the nearest Fe atom (and has two next nearest Fe neighbors), the paramagnetic dipolar interaction in our case should be larger by about a factor of 3. Thus, a paramagnetic dipolar interaction of ca. 50 kHz is plausible on structural grounds.

The biexponential T_1 obtained from relaxation time measurements suggest that two different populations of deuterons in approximately equal amounts are present in α -(PANI) FeOCl . A likely assignment is to the two *inequivalent* ring deuterons that would result in our proposed structure (Figure 6) if the aromatic rings are tilted from the “flat” position with respect to the FeOCl host. The fast-relaxing component is likely to be

(66) We note that the spectrum of the slow-relaxing component obtained by the null method is not exactly identical to what would be obtained from a hypothetical fully-relaxed spectrum of *only that slow-relaxing component*, since it is essentially obtained with an excitation profile of a 270° (composite) quadrupolar-echo “pulse” rather than that of a 90° (composite) quadrupolar-echo “pulse”. However, the spectrum of the fast-relaxing component obtained by this same method should not exhibit such a difference. Therefore, the null spectrum in Figure 10A should represent reasonably well the true spectrum of the fast-relaxing component, if the defocusing effects of paramagnetic dipolar interactions are negligible.

(67) Slichter, C. P. *Principles of Magnetic Resonance*; 3rd ed.; Springer Verlag: New York 1989.

due to the deuteron closest to the paramagnetic Fe center(s) responsible for the relaxation; the high degree of asymmetry and greater breadth of the powder pattern (due to the low-field side of the spectrum) of this fast-relaxing component are the expected consequences of a larger paramagnetic dipolar interaction. Spin-diffusion is essentially quenched in this case because the *instantaneous* resonance frequencies of any two neighboring deuterons are likely to be widely different given the different orientation of their quadrupolar and dipolar tensors.

The variable-temperature spectra strongly suggest that motion of the aromatic rings is taking place at elevated temperatures, most likely ring flips as have been observed to occur in the bulk polymer itself.⁵⁸ Even without detailed simulations, the appearance of the spectra, particularly the presence of two outer horns and the wide spectral width, suggest that most of the rings are essentially static (nonflipping) at room temperature. The temperature-dependent changes in the spectra are not affected much by changes in the magnitude of the Curie moment, since the difference in absolute temperature is so comparatively small. The static behavior of aromatic rings of intercalated PANI underscores the significant spatial confinement experienced by the polymer. Overall, the ^2H NMR results provide independent confirmation of the intimate contact between the PANI polymer chains and the FeOCl host and rule out the presence of a simple phase mixture.

Mössbauer Spectroscopy. In order to better characterize the electronic structure of FeOCl after intercalation we performed variable temperature Mössbauer spectroscopic studies. The Mössbauer spectra were recorded in the temperature range 20 – 300 K. The spectra of α -I at various temperatures enabled us to define two temperature ranges corresponding to different magnetic states in the material. Above ~ 70 K all spectra are indicative of paramagnetic behavior with localized and delocalized electrons. Below 70 K the Zeeman-splitting patterns characterize long range magnetic order within the FeOCl host.

The Paramagnetic Region of α -I. Typical Mössbauer spectra of α -I at temperatures from 89 K to room temperature are shown in Figure 11A. The spectra in this temperature region have been analyzed by fitting the experimental data to independent Lorentzians. The results of this analysis are summarized in Table 1. The spectrum at 89 K consists, clearly, of three well resolved lines. The more intense doublet is due to the majority octahedral high spin Fe^{3+} atoms of the host lattice in a paramagnetic state, while the minor peaks are assigned to octahedral host Fe^{2+} . The isomer shift of the major site at 89 K is 0.45 mm/s , which is comparable to the observed value for the pristine FeOCl at the same temperature (0.50 mm/sec at 78 K).⁶⁸ The room temperature spectrum consists readily of two well resolved lines which can be fitted also to a pair of Lorentzian lines. The individual areas under the resonance curves are equal, but the intensities and the line widths are not. The spectrum at 152 K also consists of two well resolved absorption lines which can be fit to a pair of Lorentzians with nonequal line widths, intensities, and areas.

This simple analysis of the above spectra provides the following information. First, the observation of nonequal areas at $T <$ room temperature and equal areas at room temperature may suggest that the Fe atom participates in significantly anisotropic vibrations (Goldanskii-Karyagin effect). This effect is expected to be temperature dependent, which is consistent with our experimental observation. In addition, the nonequal line widths of the absorption suggest heterogeneities in the Fe^{3+}

(68) (a) Herber, R. H. *Acc. Chem. Res.* **1982**, *15*, 216. (b) Herber, R. H.; Maeda, Y. *Inorg. Chem.* **1981**, *20*, 1409. (c) Eckert, H.; Herber, R. H. *J. Chem. Phys.* **1984**, *80*, 4526.

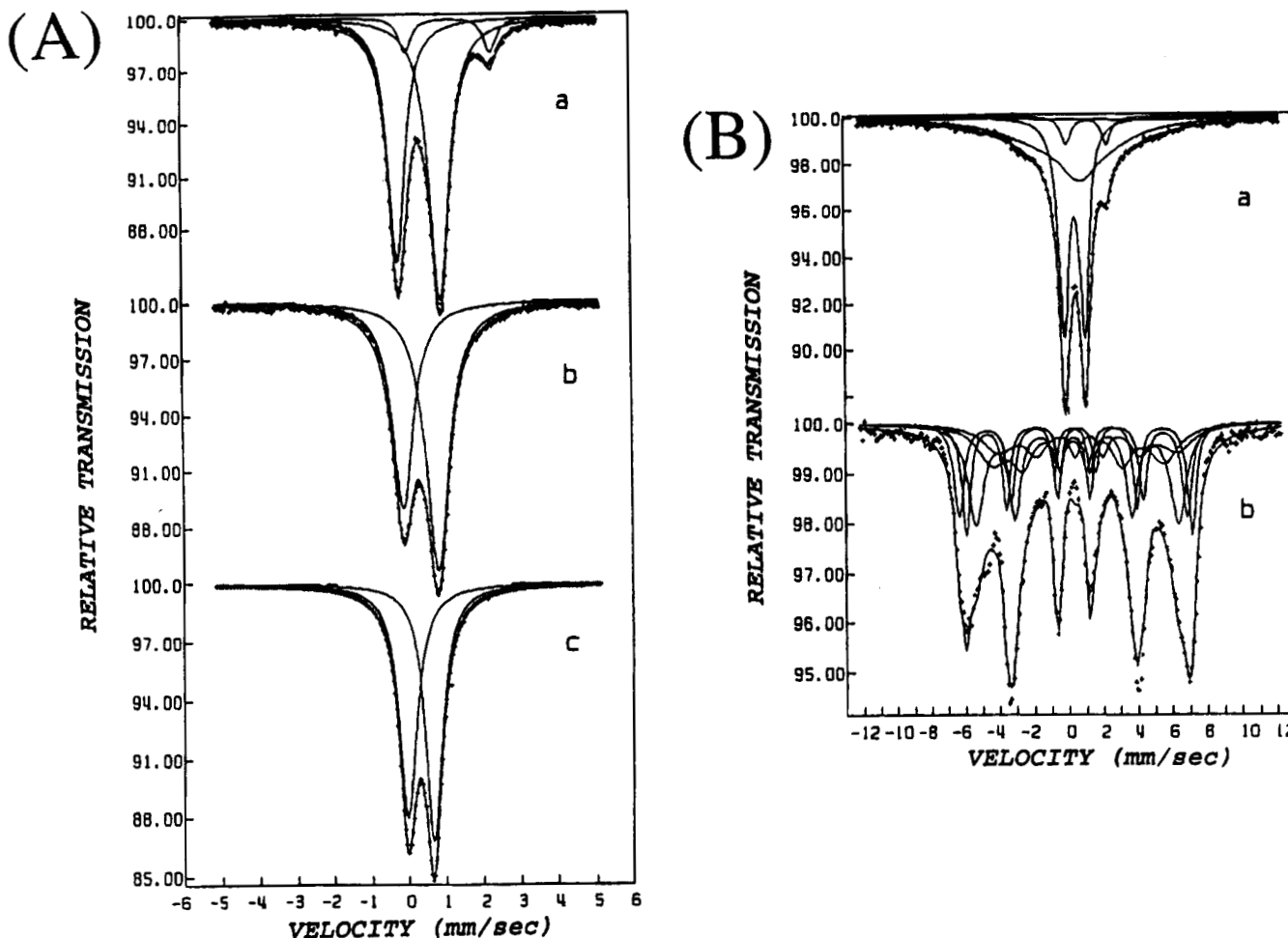


Figure 11. Temperature dependent Mössbauer spectra of α -(PANI)_{0.17}FeOCl: (A) (a) at 89 K, (b) at 152 K, (c) at 300 K, and (B) (a) at 55 K. The broad component in the center represents the beginning of a magnetically split spectrum of an Fe^{3+} site (b) at 23 K. The various components originate from slightly different Fe^{3+} sites and perhaps preferential orientation effects.

site of α -I. The temperature dependencies of the quadrupole splitting (ΔE_q) and the isomer shift (IS) parameter of the Fe^{3+} sites are not consistent with the second-order Doppler shift effect of a FeOCl lattice and may suggest that the Fe^{3+} site is picking up some Fe^{2+} character at higher temperatures, indicating a more efficient electron hopping between the two sites. The intensity ratio of the two sites (Fe^{2+} and Fe^{3+}) is approximately 1:9. This is also supported by the experimental observation that the area of the Fe^{2+} site diminishes as the temperature increases from 89 K to room temperature. The above observations are similar to those observed in other intercalated FeOCl compounds.⁶⁸ Therefore, the changes in our spectra with rising temperature in this region can be explained, at least qualitatively, with increasing delocalization of the electron between the Fe^{2+} and the Fe^{3+} sites. This is reflected in the enhanced electrical conductivity at room temperature.

The Magnetic Region of α -I. Below 70 K long-range magnetic order sets in. Typical spectra in the temperature region 70–20 K are shown in Figure 11B. Below \sim 70 K the lines of the spectra gradually start to broaden as the temperature falls and a magnetic pattern appears. In order to take into account the asymmetry and the broadness of the spectra we have analyzed these data with a minimum number of magnetic components having a distribution of hyperfine field parameters. Very broad hyperfine components are expected at temperatures very close to the Neel temperature (T_N) which is estimated to be \sim 70 K. This is typical of superparamagnetic behavior with relaxation phenomena. The T_N is substantially lower than that

of FeOCl itself (90 K).⁶⁹ Below 40 K no major changes occur in the Mössbauer spectra except that the intensity of the Fe^{2+} peak becomes weaker than at 89 K and finally at 20 K it is difficult to distinguish traces of the Fe^{2+} site. Mainly the absence of the absorption line of the paramagnetic Fe^{2+} site at \sim 2 mm/s is a clear indication that the Fe^{2+} site is becoming magnetic, but unfortunately its sextets are smeared out by the crystalline field and are hidden under the more intense Fe^{3+} spectrum. This precludes the determination of the Fe^{2+} contribution at low temperatures. The spectral pattern at 23 K is asymmetric, due to a number of factors including the presence of Fe^{2+} sites, slightly different Fe^{3+} sites, and perhaps preferential orientation effects.

β -Phase. The Mössbauer parameters of the " β "-phase are strongly suggestive of OH coordination to the Fe centers. The spectroscopic data obtained at various temperatures are summarized in Table 1. Except for an impurity phase containing octahedral Fe^{2+} sites coordinated by oxygen atoms ($\delta = 1.18$ mm/s, $\Delta E_q = 2.05$ mm/s at room temperature), the data bear remarkable resemblance to those obtained for β -FeOOH, known as the mineral akageneite (which is known to contain Cl^-).⁷⁰ This was confirmed independently by studying a pure sample of synthetic β -FeOOH. Furthermore, the new diffraction lines

(69) (a) Bizette, H.; Adam, A. *C. R. Acad. Sci. Paris Ser. B* 1972, 275, 911. (b) Halbert, T. R.; Johnston, D. C.; McCandish, L. E.; Thompson, L. J.; Scanlon, J. C.; Dumesic, J. A. *Physica B* 1980, 99, 128.

(70) (a) Watson, J. H. L.; Cardell, Jr., R. R.; Weller, W. *J. Phys. Chem.* 1962, 66, 1757. (b) Mackey, A. L. *Mineral Mag.* 1960, 32, 545–557. (c) Mackey, A. L. *Mineral Mag.* 1962, 34, 270.

Table 1. Temperature Dependence of Isomer Shift (IS) and Quadrupole Splitting (ΔE_q) for α - and " β "-(PANI)_{0.17}FeOCl

material	temperature (K)	IS(mm/s)	ΔE_q (mm/s)
α -(PANI) _{0.17} FeOCl	RT ^a	0.42	0.70
	152	0.44	0.93
	89	0.45	1.07
		1.26	2.27
	55	0.45	1.20
		1.25	2.30
	23	0.45	0.16 ^b
β -phase		1.23	-1.5
	RT ^a	0.33	0.72
	233	0.37	0.78
	182	0.35	0.80
	149	0.38	0.84
	58	0.43	0.85
	23	0.46	-0.18 ^b

^a Room temperature is abbreviated RT. ^b Totally split magnetic spectra.

appearing in the XRD pattern of " β "-I are consistent with akageneite. Thus the inorganic framework has been transformed to β -FeOOH, and the so-called " β "-phase is actually a highly intimate mixture of PANI and β -FeOOH. This probably occurs from the slow and continuous hydrolysis/oxidation of α -I in ambient environment, which also has the effect of further polymer chain coupling of PANI molecules. The formation of β -FeOOH upon air oxidation of α -(PANI)_xFeOCl was recently observed by inelastic neutron scattering experiments.⁷¹

Electron Paramagnetic Resonance (EPR) and Magnetic Susceptibility. The EPR spectra of α -(PANI)_xFeOCl are very broad and too complex to be of real characterization value. We examined these spectra in order to see whether we could observe the typical EPR $S = \frac{1}{2}$ singlet of PANI (emeraldine salt). Interestingly, the characteristic sharp EPR polaron signal did not show up in α -I, presumably due to exchange broadening with the paramagnetic FeOCl layers. In a control experiment, finely divided mixtures of (PANI)Cl/FeOCl and (PANI)Cl/ α -I did show the narrow characteristic $S = \frac{1}{2}$ signal of PANI at $g = 2.0023$. The absence of a PANI signal from the α -I phase indicates that the polymer is closer than ~ 15 Å to the paramagnetic FeOCl layer and confirms the notion that this material is a pure intercalation compound and not a phase mixture in which bulk PANI is one of the components.

Variable temperature magnetic susceptibility data for α -I are similar to those of FeOCl except for a low temperature Curie tail.⁶⁹ This suggests that the short range antiferromagnetic interactions observed in FeOCl are also present in α -I. The spin-only magnetic moment (μ_{eff}) of α -I is $2.8 \mu_B$ at room temperature, which is slightly higher than that of FeOCl, but much lower than the theoretical high-spin Fe^{3+} ($5.9 \mu_B$) or Fe^{2+} ($4.9 \mu_B$) values.

Charge Transport Properties. Electrical Conductivity. Samples of α -I were studied in pressed pellet and single crystal form by ac and dc electrical conductivity measurements using the four-probe geometry. Room temperature conductivities for pressed pellets and single crystals of several (PANI)_xFeOCl samples range between 0.01 and 0.1 S/cm. We found, by X-ray diffraction, that in pressed pellets significant orientation effects are present which cause the crystallites to orient with their crystallographic ac-planes perpendicular to the pressing axis. Thus, the measurements were essentially carried out parallel to the ac-planes. Interestingly, the observed conductivities of the pressed pellets were not dramatically lower than those obtained from single crystal samples, as is the case for other conducting

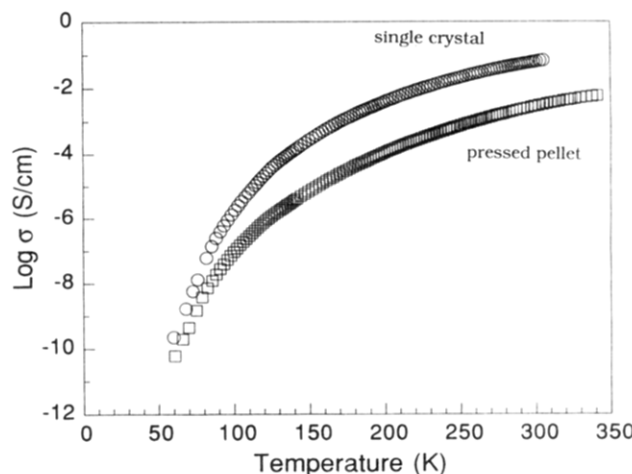


Figure 12. Four-probe variable temperature electrical conductivity data for α -(PANI)_{0.20}FeOCl in pressed pellet and single crystal form.

compounds. Figure 12 shows the temperature dependence of the electrical conductivity of α -I in pressed pellet and single crystal form. The latter, at 0.15 S/cm, is only 10 times greater than the polycrystalline pellet at room temperature, although at lower temperatures this difference becomes greater. A significant feature of the single crystal data is the thermally activated temperature dependence of the conductivity, suggesting that the material is a semiconductor. The thermally activated conductivity of single crystals of α -I may be due to several factors, including domain boundaries in the crystals due to fracture upon intercalation and, most likely, the finite length of PANI chains in the intralamellar space, which could generate large activation barriers for carrier hopping from chain end to chain end.

Overall, the electrical conductivity of α -I is lower than that of bulk PANI films by approximately two orders of magnitude. This could be due to the differences in morphology between the two samples (films of PANI are smoother and more continuous), differences in carrier density per unit volume in bulk PANI compared to α -I, which is only $\sim 15\%$ PANI by weight, and the lower molecular weight of PANI in α -I. Furthermore, the significantly shorter polymer chain length in α -I than that in bulk PANI necessitates more frequent carrier hopping from chain-end to chain-end in α -I.

Compound α -I has an order of magnitude lower conductivity than (Ppy)_{0.34}FeOCl and (Pth)_{0.24}FeOCl.³¹ This parallels the trend observed in the corresponding bulk samples, where PANI is less conductive than either polypyrrole or polythiophene. However, α -I is significantly more conductive than other FeOCl intercalation compounds containing molecular guests.^{34,35} For example, samples of (pyridine)_{0.33}FeOCl, (ferrocene)_{0.5}FeOCl, and (TTF)_{0.125}FeOCl display maximum conductivities at room temperature of 10^{-3} S/cm. Charge transport in these compounds is due to the Fe^{2+}/Fe^{3+} mixed valency in the reduced FeOCl layer. The electrical conductivity of reduced FeOCl is due to the small but finite mobility of 3d electrons in Fe^{2+} and Fe^{3+} in FeOCl slabs. By comparison, pristine FeOCl (all Fe^{3+}) is an insulator. Since FeOCl layers alternate with PANI in α -I the overall conductivity will be limited by the ability of the carriers to move in a direction perpendicular to the layers. This mobility is greater in a direction parallel to the layers, which makes α -I a very anisotropic material. The true conductivity of the confined PANI chains is difficult to assess, but it is expected to be much higher than the observed values. Attempts to extract the PANI chains from α -I by dissolving the inorganic framework in HCl and still keep them oriented failed. Instead an amorphous polymer with a conductivity of 0.1 S/cm was obtained.

(71) Prassides, K.; Bell, C. J.; Dianoux, A. J.; Wu, C.-G.; Kanatzidis, M. G. *Physica B* **1992**, 180&181, 668.

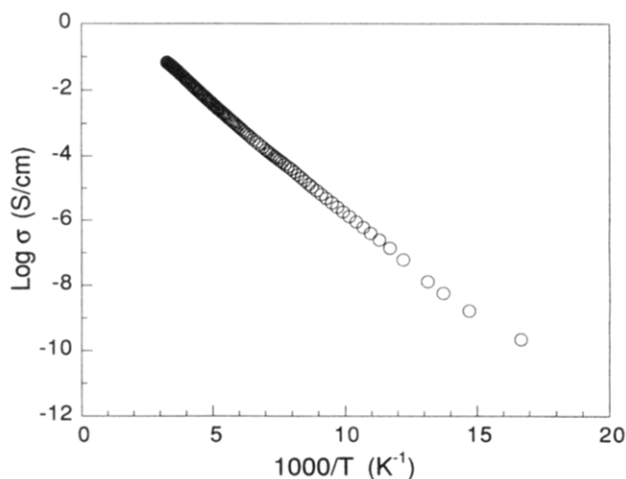


Figure 13. Pressed pellet four-probe variable temperature electrical conductivity for “ β ”-(PANI)_{0.17}FeOCl.

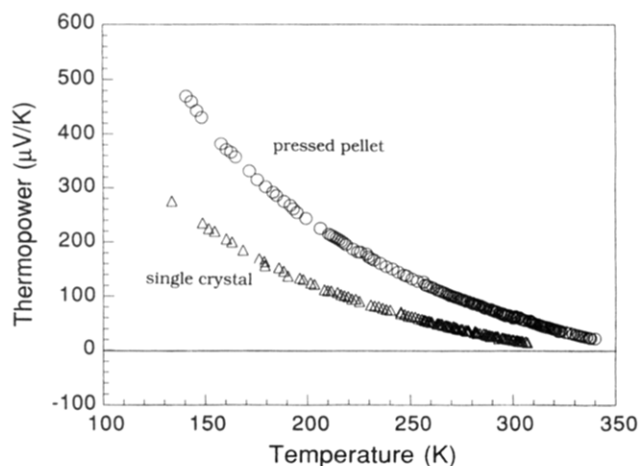


Figure 14. Variable temperature thermoelectric power data for a single crystal and pressed pellet of α -(PANI)_{0.17}FeOCl. The data have been corrected for the contribution of the gold electrodes.

The conductivity of “ β -I is ten times higher than that of α -I at all temperatures, see Figure 13. This suggests the presence of longer chains of PANI in the oxidized product. The IR spectra, solubility, thermal, and GPC data support this hypothesis. Supporting evidence comes from the comparison of the conductivity of PANI extracted from α -I and the “ β ”-phase. Consistent with longer chain lengths in β -PANI its electrical conductivity is 100 times higher than that from α -I.

Thermoelectric Power Studies. The conductivity measurements alone cannot unequivocally characterize the electrical behavior of a polycrystalline sample. A complementary probe to address the charge-transport issue is thermoelectric power (TP) measurements as a function of temperature. TP measurements are typically far less susceptible to artifacts arising from the resistive domain boundaries in the material because they are essentially zero-current measurements. This is because temperature drops across such boundaries are much less significant than voltage drops. Figure 14 shows typical TP data for α -I and “ β ”-I as a function of temperature. Accurate measurements at low temperatures were hindered by the very large sample resistances that developed.

The room temperature TP of α -I is slightly positive (close to zero) and increases steadily with decreasing temperature, reaching the value of 100–400 $\mu\text{V}/\text{K}$ at 150 K. Single crystals of α -(PANI)_xFeOCl show similar behavior. This is characteristic of a p-type semiconductor, similar to that observed for (ferrocenium)_{0.50}FeOCl⁷² but different from (Ppy)_{0.34}FeOCl and

(Ph)_{0.24}FeOCl,³¹ which show p-type metallic character. Since the emeraldine salt of PANI shows metal-like TP behavior,⁷³ we can conclude that in α -(PANI)_xFeOCl the reduced FeOCl framework dominates the charge transport properties. This can be explained by the presence of short PANI chains in the interlayer space that impede chain to chain charge transport by introducing too many carrier hopping barriers, thus making charge transport through FeOCl layers (via $\text{Fe}^{2+}/\text{Fe}^{3+}$ exchange) more favorable. Interestingly, the TP behavior of the “ β ”-phase is dramatically different. The Seebeck coefficient is negative in this case, indicating a conductivity change from p-type to n-type, with typical values of around $\sim 2 \mu\text{V}/\text{K}$, similar to the conducting form of bulk PANI. Since β -FeOOH is an insulator, the TP data reflect the conductive properties of the PANI component and are in agreement with our other experimental evidence that this phase is actually an intimate mixture of PANI and β -FeOOH.

Concluding Remarks

Conducting PANI (emeraldine salt) was formed inside FeOCl by an *in situ* oxidative polymerization/intercalation reaction between aniline and FeOCl. The rate of reaction under air is faster than under nitrogen because, in addition to FeOCl, molecular oxygen acts as an electron (and proton) acceptor. The degree of reduction of the FeOCl is 0.1e/mol. The resulting moisture-sensitive, crystalline, α -(PANI)_xFeOCl consists of alternating monolayers of conducting polymer and inorganic framework FeOCl and is a p-type semiconductor with a room temperature electrical conductivity of $10^{-2} \text{ S}/\text{cm}$. The ²H NMR spectra of the perdeuterated samples arise predominantly from the aromatic ring deuterons, and the rings do not appear to undergo “ring flips” to a significant extent at room temperature or below. This is in contrast to bulk PANI, which does undergo “ring flips”, and confirms that in the FeOCl galleries the polymer is experiencing significant host-imposed motional restrictions. Intralamellar polymer growth is restricted and slow, yielding considerably shorter PANI chains than those grown in an unrestricted fashion, but the intercalated polymer exhibits narrower chain polydispersity. The PANI chain-length inside the FeOCl layer continues to grow with time in the presence of ambient oxygen. At the same time hydrolysis of the FeOCl framework occurs to yield β -FeOOH. The polymer chain growth suggests that oxygen may help polymerize various oligomers or monomers into polymers inside structurally confined environments. In several cases this has now been demonstrated.^{26b,74} The PANI/FeOCl system is the first polymer intercalation compound in which substantial polymer ordering, “endotaxy”, is observed inside a host material.

Acknowledgment. Financial support from the National Science Foundation (DMR-93-06385) is gratefully acknowledged. M.G.K. is a Camille and Henry Dreyfus Teacher Scholar 1993–1995. At NU this work made use of Central Facilities supported by NSF through the Materials Research Center (DMR-91-20521). The NMR data were obtained on instrumentation housed in the Max T. Rogers NMR Facility at Michigan State University. This work made use of the SEM facilities of the Center for Electron Optics at Michigan State University. J.P.Y. thanks the Office of Naval Research for partial support.

JA943938Z

(72) Villeneuve, G.; Dordor, P.; Palvadeau, P.; Venien, J. P. *Mater. Res. Bull.* **1982**, 17, 1407.

(73) (a) Park, Y. W.; Lee, Y. S.; Park, C. *Solid State Commun.* **1987**, 63, 1063. (b) Zuo, F.; Angelopoulos, M.; MacDiarmid, A. G.; Epstein, A. J. *Phys. Rev.* **1987**, B36, 3475.

(74) Liu, Y.-J.; Kanatzidis, M. G. Manuscript in preparation.